Evaluation of Rapid Manufacturing Solutions for Improved Knee Implants using Finite Element Analysis

P. Vinay kumar

A Dissertation Submitted to
Indian Institute of Technology Hyderabad
In Partial Fulfillment of the Requirements for
The Degree of Master of Technology

भारतीय प्रौद्योगिकी संस्थान हैदराबाद
Indian Institute of Technology Hyderabad

Department of Mechanical Engineering

July, 2012

Declaration

I declare that this written submission represents my ideas in my own words, and where others ideas or words have been included; I have adequately cited and referenced the original sources. I also declare that I have adhered to all principles of academic honesty and integrity and have not misrepresented or fabricated or falsified any idea/data/fact/source in my submission. I understand that any violation of the above will be a cause for disciplinary action by the Institute and can also evoke penal action from the sources that have thus not been properly cited, or from whom proper permission has not been taken when needed.

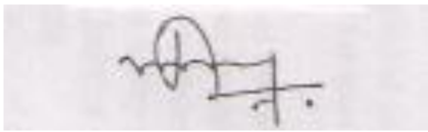

(Signature)

P. Vinay Kumar

ME10M06

Approval Sheet

This thesis entitled "Evaluation of Rapid Manufacturing Solutions for Improved Knee Implants using Finite Element Analysis" by P.Vinay Kumar is approved for the degree of Master of Technology from IIT Hyderabad.

Dr. Abhay Sharma
Assistant Professor
Department of Mechanical Engineering
Examiner

Dr. Raja Banerjee
Assistant Professor
Department of Mechanical Engineering
Examiner

Dr. S. Surya Kumar
Assistant Professor
Department of Mechanical Engineering
Adviser

Dr. Suhash Ranjan Dey
Assistant Professor
Department of Material Science and Engineering
Chairman

Acknowledgements

It is a great experience and learning for having worked with one of the country's premier institute of technology, IIT Hyderabad. It's a memorable journey for me to evaluate myself professionally which helped in overall self-development. For now, it gives me an immense pleasure to thank the great minds behind my successful completion of M. Tech Thesis work.

I am so grateful to my thesis guide **Dr. S. Surya Kumar**, Assistant Professor, Department of Mechanical Engineering, for providing excellent guidance, consistent encouragement, inspiration and motivation to stay focused throughout the research work. Without his invaluable guidance, this work would never have been a successful one.

I also wish to thank **Prof. Dr. Eswaran Vinayakan**, H.O.D, Department of Mechanical Engineering, and **Professor U.B Desai**, Director, IIT Hyderabad for providing us with the necessary infrastructure and the professional support at all times.

I want to thank **Mr. Guru Prasath Ravindran** (Project Associate), Ph.D scholar's **Md. Kushafudoja** and **Somashekara M.A** Department of Mechanical Engineering for the fruitful discussions.

I would like to extend my gratitude to all the faculty members for their care and support which helped us grow our attitude and character along with the professional skills

I would like to thank Staff members of the Institute, Project Associate Staff of CAE Lab and Manufacturing Lab, Research scholars and M Tech colleagues of Department of Mechanical Engineering for their help and support, whenever needed.

I am also thankful to all my friends at IIT Hyderabad, especially M. Tech Design Engineering students, for providing a stimulating and fun environment and making my stay in the institute campus a pleasure and also helping me in all the ways professionally and personally.

Dedicated to

My beloved Father Late. Sri P. Vijay Kumar

&

Mother Sri P. Florence

&

My Wife P. Karuna Vinay

&

all my Family Members.

Abstract

Knee joint is an important part of human body; failure of knee joint may occur mainly because of surface to surface contact of femoral and tibial surfaces owing to the dry out of bursae fluid. The damaged surfaces must be replaced by artificial implants made of metals, ceramics, or composite materials. This process is known as total knee replacement.

Three-dimensional physical model of the knee implant is modeled in NX Unigraphics 7.5 software. This model is imported to ANSYS-WORKBENCH 13, solver used is MECHANICAL-APDL, which is based on Finite Element Method (FEM).

The metallic implant is made of porous inside and dense outside. This reduces the overall weight of the implant. The failure of bearing component in knee implant is due to high stresses at the contact regions of femoral component and polyethylene insert causes wear and decreases the life of the implant. New improved knee joint implant is made, which reduces the stresses at the contact regions and increases the life of knee implant. The stiffness of artificial implants is around 110 GPa to 210 GPa, while that of the human bone is around 17 GPa. A metallic implant made of titanium-β alloy having stiffness of around 40 GPa to 60 GPa is used. This reduces the effect of stress shielding between the bone and implant.

Nomenclature

E – Young's Modulus

A – Cross sectional area

q – Force per unit length

σ – Stress

$\sigma_x, \sigma_y, \sigma_z$– Stresses in x, y, z directions

ϵ – Strain

$\in_x, \in_y, \in_z$ – Strains in x, y, z directions

τ– Shear stress

$\tau_{xy}, \tau_{yz}, \tau_{xz}$– Shear stresses in xy, yz, xz directions

γ – Shear strain

$\gamma_{xy}, \gamma_{yz,} \gamma_{xz}$ – Shear strains in xy, yz, xz directions

D – Elastic constant

u, v, w – Displacements in x, y, z directions

n_x, n_y, n_z – Normal vectors in x, y, z directions

Contents

List of Figures

List of Tables

Chapter 1

Introduction

Rapid Prototyping (RP), also known as Additive Manufacturing (AM), is a totally automatic process of manufacturing objects directly from their CAD models. With the help of RP technology 3D models can be easily generated an a layer by layer deposition process. The 3D CAD data is sliced into 2D layers and realized one layer at a time, making it simple to construct a 3D model and manufacture.

In any manufacturing industry, time for the product manufacturing and surface finishing of the product are some of the main criteria. There are many manufacturing processes such as casting, molding, machining, etc. to manufacture the product in less time and with good surface finish. However, these traditional methods are incapable of producing more complicated geometries. Rapid Prototyping and Manufacturing technologies offer better advantages in terms of less product development time, shape complexity and ability to realize objects with gradient properties. Owing to these reasons, RP methods are generating interest in the biomedical field including total knee replacements.

1.1. Rapid Prototyping Processes

There are various RP processes which are used to fabricate 3D models. The following are some RP processes which are commonly used.

1. Stereolithography,
2. Selective laser sintering,
3. 3D printing,
4. Laser Engineered Net Shaping,
5. Fused Deposition Modelling,

1.1.1 Stereolithography (SLA):. SLA process was developed by 3D system Inc, of Valencia, USA in the year 1986. The technique builds 3D models from liquid photosensitive polymers that solidify when exposed to ultraviolet light. As shown in the Figure 1.1, the model is built upon a platform situated just below the surface in a vat of liquid epoxy or acrylate resin. A low-power highly focused UV laser traces out the first layer, solidifying the model's cross section while leaving excess areas liquid. Next, an elevator incrementally lowers the platform into the liquid polymer. A sweeper re-coats the solidified layer with liquid, and the laser traces the second layer atop the first. This process is repeated until the prototype is complete. Afterwards, the solid part is removed from the vat and rinsed clean of excess liquid. Supports are broken off and the model is then placed in an ultraviolet oven for complete curing.

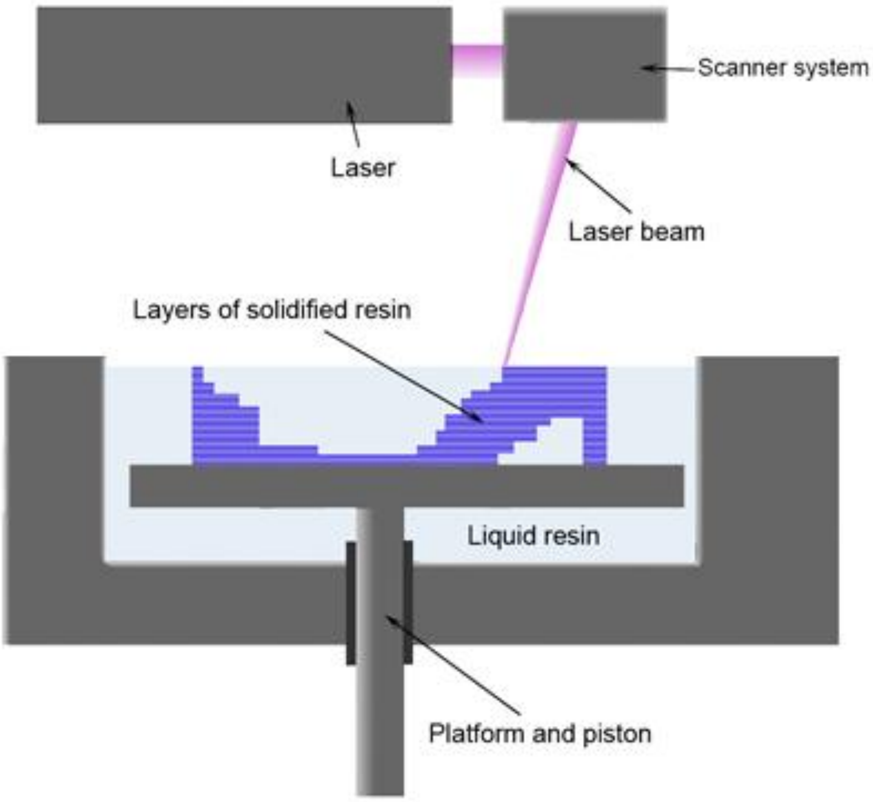

Figure 1.1: Stereolithography process
[http://en.wikipedia.org/wiki/File:Stereolithography_apparatus.jpg]

a) **Material:** 3D systems Inc. of Valencia, USA uses Acrylate-Photopolymer or Epoxy resin for making a physical model.

b) Applications: SLA has many applications in the various industries as shown in the Figure 1.2

(a) Gun used in military

(b) Manifold of automoble engine

(c) Aluminium fan

(d) Skull

Figure 1.2: Applications of SLA

c) Strengths:

i. Accuracy is high.
ii. Good surface finish.
iii. Capable of high detail and thin walls.

d) Weaknesses:

i. Removing of support structure is difficult.
ii. The material used in this process is toxic and hazardous.

1.1.2 Selective laser Sintering (SLS): Selective laser sintering process was patented in the year 1989 and developed by Carl Deckard for his master's thesis at the University of Texas. SLS machines are produced by DTM Co, Texas. The process is shown in the Figure 1.3. SLS creates 3D models. The 3D parts are built upon a platform which sits just below the surface in a bin of the heat-fusible powder. A laser traces the pattern of the first layer, sintering it together. The platform is lowered by the height of the next layer and powder is reapplied with the help of a roller. This process continues until the part is complete. Excess powder in each layer helps to support the part during the build.

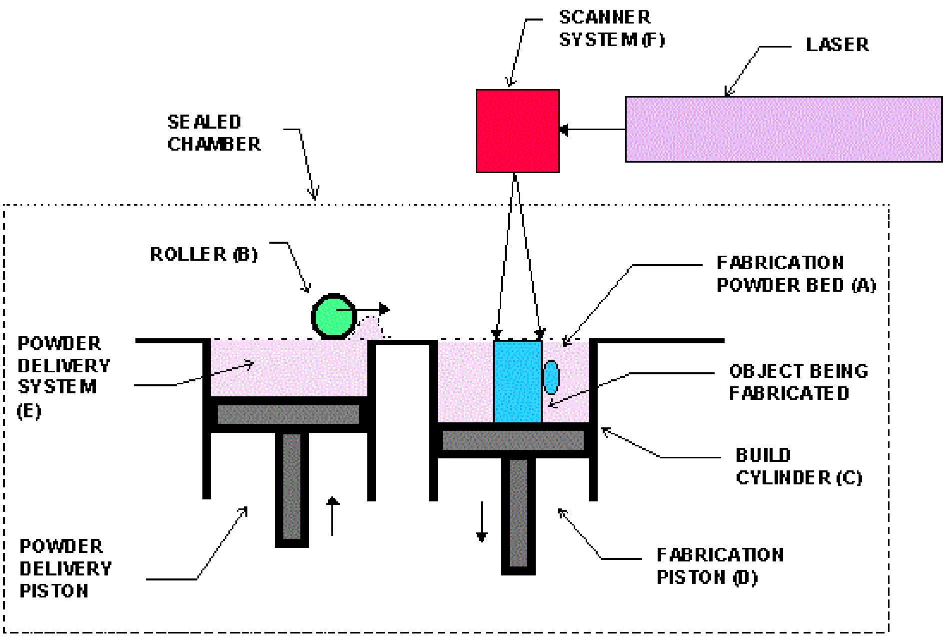

Figure 1.3: Selective laser sintering process
[http://www.additive3d.com/sls.htm]

a) **Material:** In this process the materials used for creating 3D models by using the laser beam to fuse selectively are Polycarbonate or Glass filled composite nylon, Elastomer, Low carbon steel, Polymer coated metals.

b) Applications: SLS process has vast applications in fabricating 3D models, such as in the medical field, automobile industry, manufacturing industries, etc. Some of the applications are shown in the Figure 1.4

(a) Vehicle mould

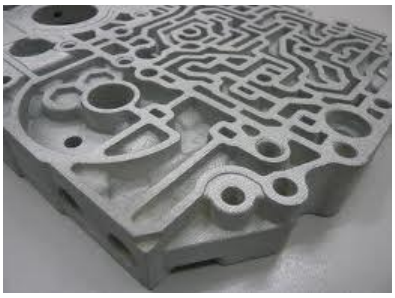

(b) Casting mould

(c) Water pump part

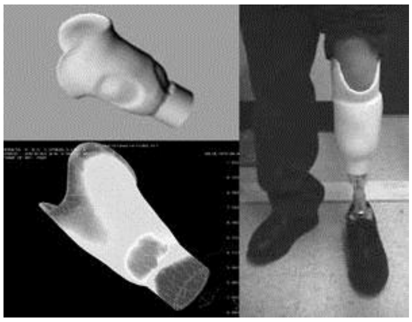

(d) Water pump part

Figure 1.4: Applications of SLS process

c) Strengths:

i. The parts which are made by this process are tough.
ii. No support structures are required.
iii. No post curing is requiring.
iv. There is no wastage of material.

d) Weaknesses:

i. The parts are porous in nature.
ii. Surface finish is not so good.
iii. The parts made by this process are brittle.

1.1.3 3D Printing: 3D printing process was developed at the MIT. In 3D printing, the part is build up in a bin that is fitted with a piston to incrementally lower the part into the bin. The process is shown in the Figure 1.5, which explains the process. The powder is dispensed from a hopper above the bin and a roller is used to spread and level the powder. An inkjet printing head scans the powder surface and selectively injects a binder into the powder, which is used to join or bind the powder. The unbound powder becomes the support material. After building the model completely, the green structure is fired and the model is removed from the unbound powder. This process is very fast and produces parts with slightly grainy surface.

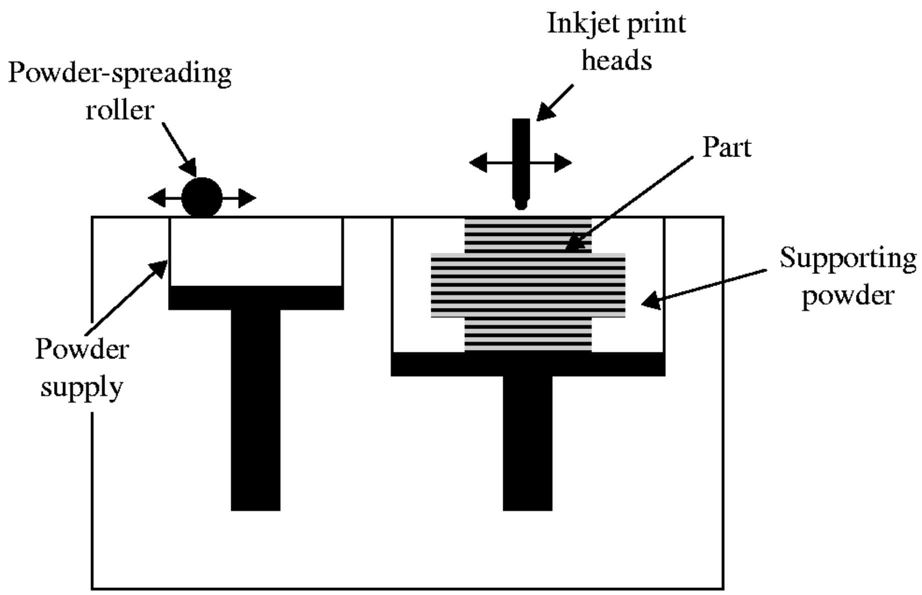

Figure 1.5: 3D printing process
[http://www.xpress3d.com/Zcorp3DP.aspx]

a) **Material:** Powder based material such as Alumina is used. Colloidal silica is used as a binder. Polypropylene is used which is having high strength, flexible and durable. Rubber is also used in this process. Dental wax follow up materials are also used in dental applications.

b) Applications: SLS process has vast applications in fabricating 3D models, such as in the medical field, automobile industry, manufacturing industries, etc. Some of the applications are shown in the Figure 1.6

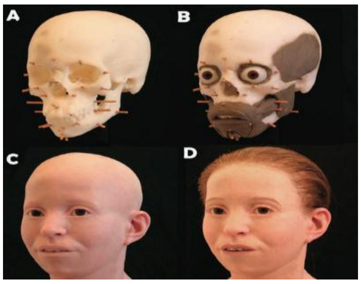

(a) Facial prosthetic

(b) Fuel injection pump

(c) Head phones

(d) Aeroplane prototype

Figure 1.6: Applications of 3DP process

c) Strengths:

i. Functional metal parts can be obtained directly.
ii. No external support structures are required.

d) Weaknesses:

i. Poor surface finish.
ii. Post curing is required.
iii. Parts are likely to be porous.

1.1.4 Laser Engineered Net Shaping (LENS): The method is developed at Sandia National Labs and commercialized by Optomec. POM Group, Accufusion Inc.

In this process a high power laser is used to soften metal powder. The deposition head is surrounded by 2 or 4 nozzles which carries powder as shown in the Figure 1.7. The laser beam travels through the centre of the head and is focused to a small spot by one or more lenses. In this process, the table moves in raster fashion to deposit each layer of object. The head is moved up vertically as each layer is completed. Metal powders deposits either by gravity, or by pressurized carrier gas. The inert gases are used for shielding purpose to protect from atmospheric oxygen.

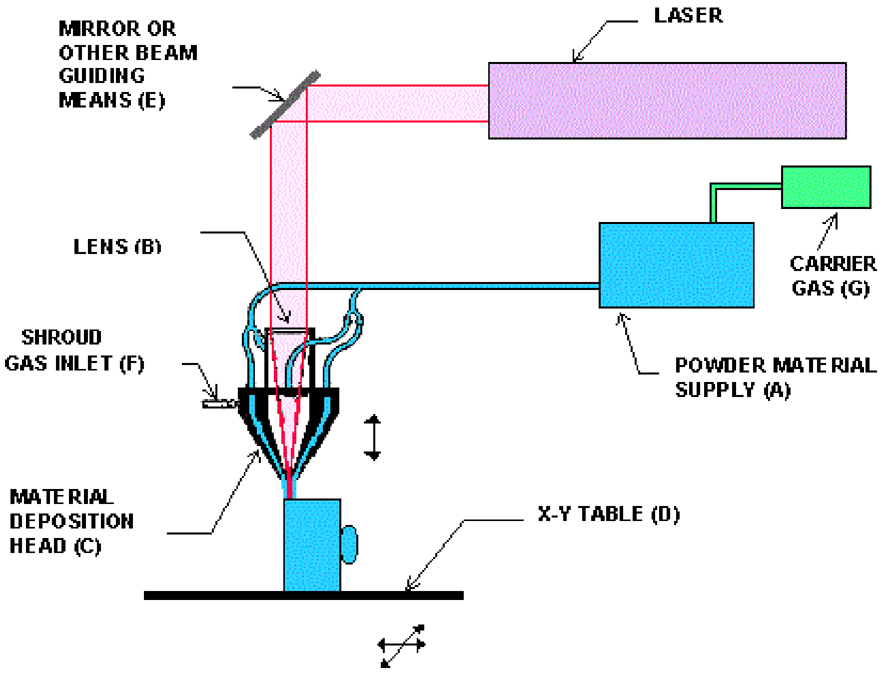

Figure 1.7: LENS process
[http://www.additive3d.com/lens.htm]

The building area is usually contained within a chamber both to isolate the process from the ambient surroundings and to shield the operators from possible exposure to fine powders and the laser beam. The laser power used varies greatly, from a few hundred watts to 20KW or more, depending on the particular material, feed-rate and other parameters.

a) Material: A variety of materials can be used such as stainless steel, Inconel, copper, aluminium and titanium.

b) Applications: Some typical applications are the fabrication and repair of injection molding tools and the fabrication of large titanium and other exotic metal parts for aerospace applications are shown in Figure 1.8. The emphasis on these applications is partly due to the fact that support structures for overhanging sections generated by the technology are fully dense and hard to remove.

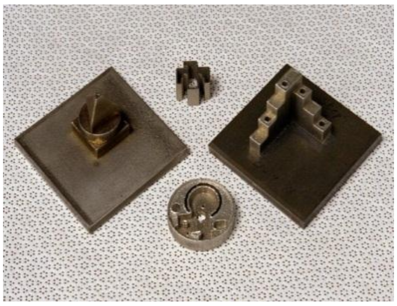

(a) Sample work pieces using LENS

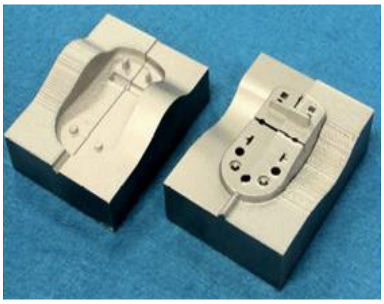

(b) Pair of mould using LENS

(c) LENS used for refurbishing a turbine

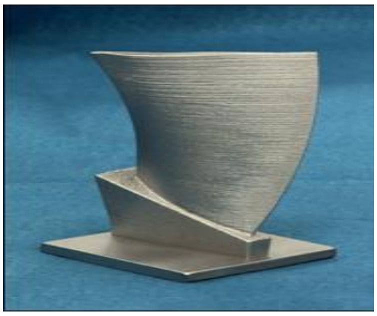

(d) Turbine Blade using LENS

Figure 1.8: Applications of LENS

c) Strengths:

i. No post curing is required.

ii. Fully dense parts with good grain structure.

d) Weakness:

i. LENS fabricated models require finishing.

ii. Material limitation.

iii. Support structures are required.

1.1.5 Fused deposition modeling (FDM): This technology was developed by Stratasys Inc, of Eden Prairie, USA. FDM is used to create the 3D models by selectively depositing a continuous filament of a thermoplastic polymer or wax through a resistively heated nozzle. The process of FDM is shown in the Figure 1.9. The machine has a XY table at the top. The XY table carries a twin-extrusion head which it can be moved in the XY plane along the desired path at the desired speed. The XY table and the platform are inside an insulated cabin whose temperature is to be maintained by the heating coils. The user can set the required temperature depending on the material used for extrusion. Generally the temperature is set a little above the melting point of the material. During the extrusion, a stream of thin filament of the semisolid material comes out of the nozzle. Its diameter is same as that of that of nozzle. Any layer is obtained by depositing the filament along its counters and filling the interiors of these counters by this filament in a zigzag fashion similar to metal cladding using a welding gun. As the material is deposited on the platform, the platform lowers and next on the previous layer again the material is deposited. This process continues until the model is created.

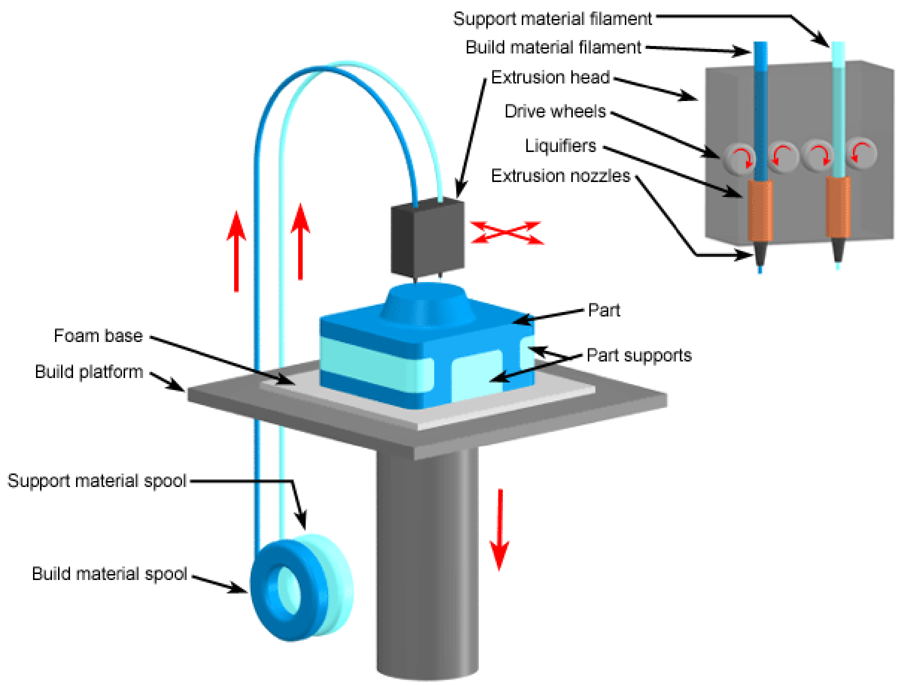

Figure 1.9: Fused Deposition Modeling process
[http://www.custompartnet.com/wu/fused-deposition-modeling]

a) **Material:** Materials include Acrylonitrile Butadiene Styrene (standard and medical grade), elastomer (96 durometer), Poly-carbonate, Polyphenolsulfone, and Investment casting wax.

b) **Applications:**

(a) Adjustible spanner

(b) Lowr jaw

(c) First aid box

(d) Children's bycycle

Figure 1.10: Applications of FDM

c) **Strengths:**

i. The machine cost is less.
ii. Ease of operation.
iii. Variety of materials can be used and the material changeover which involves only changing the head.
iv. No post-curing is required.

d) **Weaknesses:**

i. Accuracy and the surface finish is less.
ii. Strength is low in the Z-direction.

A study conducted by Milan *et al.* [1] in 2011 reported in that about 800,000 knee joint replacements are carried out per year worldwide. Total Knee Replacement (TKR) may further increase in future because of its quality and higher life expectancy. TKR may cover Tibial component, Femoral component, Patella or Knee cap. The early wear of meniscus due to dry out of bursae fluid in the knee joint causing surface to surface contact between Tibia and Femur. And failure of the knee joint one of the causes of TKR. TKR may also become necessary because of an accident.

Many implants have been used by many researchers to replace the damaged knee joint. The metallic implants which are used in knee implant surgery must have some properties, such as biocompatible in nature, non-corrosive, non-allergic. The following are some of the metallic implants used for the same:

- Titanium alloys,
- Stainless Steel 316L alloy,
- Cobalt Chromium alloys,
- Hybrid materials

Femoral and Tibial components are made up of metal, whereas the component between Femoral and Tibial component is made up of *Ultra High Molecular Weight Polyethylene* and it is called as Bearing component which provides cushioning effect.

Stress analysis using Finite Element Methods is used by many researchers to determine the stresses in the implant at the contact points (femur and bearing component) and in between the bone and the implant.

1.2. History: Total Knee Replacement

Knee implants are designed to replace biological parts that have been damaged. The first knee implant model was developed in late 1950's by Mckeever [2][3]. The implant model is Tibial Plateau Prosthesis consisted of a single metal component. The components of knee joint are shown in Figure 1.11.

Two design approaches are introduced in the late 1960's to create the knee implants. They are anatomical and functional models. Anatomical models are planned to preserve and evade the posterior cruciate ligament (PCL) and the anterior cruciate ligament (ACL) if it is engaged. The fixed surface of anatomical designs contains a cut-out slot that provides a passageway through the joint for the cruciate ligaments. Functional designs allowed non-anatomical joint surface geometries anticipated to maximize surface area and reduce polyethylene stress [4].

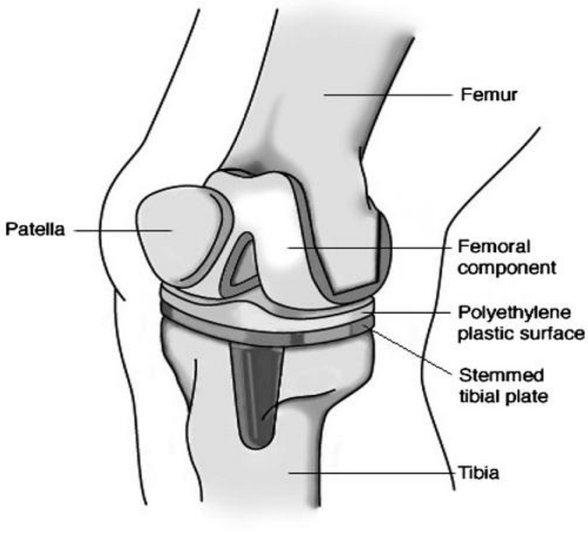

Figure 1.11: Knee implant components [5]

Buechel and Pappas developed the first mobile bearing knee implant in 1977. It was a functional design that was the prototype for their New Jersey Low Contact Stress (NJLCS) knee model [5]. This was the first rotating tibial component developed in a total condylar knee design.

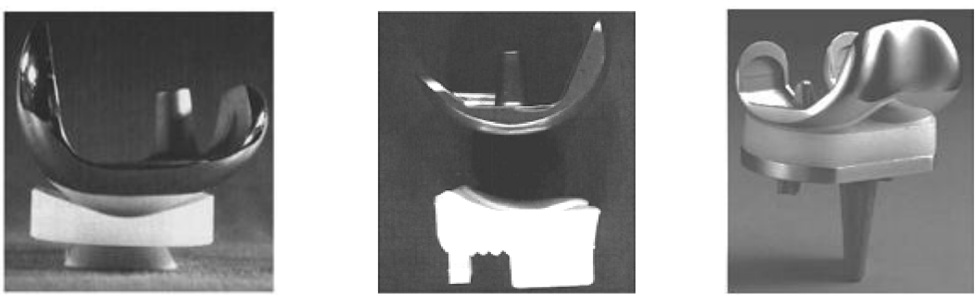

a) The Freemen-Swanson knee b) The Geomedic knee c) The Eftheker Mark II knee

Figure 1.12: Knee implant models [3]

In the late 1960's, the Freeman-Swanson established a cemented condylar total knee. This was the first cemented joint. The Geomedic knee was a originator for some of the anatomical knee models invented in 1971 by a team of engineers and physicians, it is known as the first cemented bicondylar knee design stabilizing the cruciate ligaments. The first cementless total condylar knee, the Kodama-Yamamoto Mark I knee, was invented by Yamamoto and Kodama in 1968. In 1973 Eftekhar introduced another innovation to knee implant design called as Mark II knee. This functional model was the first to have a tibial peg for fixation. The Mark II design marked the beginning of modular component usage for condylar total knees, but Robinson described the Total Condylar (TC) knee as the first truly successful and widely used functionally designed cruciate sacrificing implant [4]. About a decade later, the first porous coated total condylar knee was invented by Hungerford, Kenna and Krackow. The porous coated anatomical (PCA) knee was invented in 1979 used a coating of cobalt chrome beads on the femoral component, which also contained pegs to be embedded into the femur for stability. At least 150 types of knee implant models are currently available worldwide, and in the United States, there are about 500,000 knee replacements annually [6]. As these inventors developed their models, they used theoretical and experimental methods to improve their models. Finite element analysis has been used extensively to determine how the knee joint will respond to cyclical, impulsive and other types of loading conditions [7].

1.3. Motivation

Failure parts of the human body such as hip joint failure, knee joint failure, etc. are replaced by artificial components. Osteoarthritis, Rheumatoid arthritis, Traumatic Arthritis is common diseases in knee joint which leads to failure of the knee joint. The failure knee joint is replaced with the artificial knee components which are made of different materials. The first commercial knee implant model was developed in 1950's which is made of metal. Knee replacement surgeries are increasing day by day. With the increase of knee replacement surgeries and advancements in engineering technology, various models are designed to meet the requirements of the patient.

The following factors motivated to propose a new knee implant model in total knee replacement surgery:Presently, knee joint failures are increasing day by day because of lack of healthy food reduces the strength of bone, major accidents, lack of rest, pollution, etc. Knee joint is one the major joint in the human body. In knee joint surgery, metals are used to replace damaged surfaces. The metals are having high young's modulus and density compared to the human bone. This causes bone wear and tear, malalignments in the knee joints, stress shielding in the knee joint.

Fabrication of the knee implant is another important factor. The knee implants are fabricated by commercial processes such as casting, machining, etc. These processes take more time, and increases cost. Rapid prototyping technology is emerging favourite in the field of medicine to fabricate the bio-medical implants with in less period of time. This will reduce the risk of surgery, cost and time. With the development of new technologies in RP, the anatomical parts are fabricated effectively. Laser based processes like LENS are have the capability of fabricating such models [8]. Arc based models with similar capabilities are also under development [9].

1.4. Objective of study

The objective of the study to propose a new knee implant model in knee joint replacement surgery. The implant is designed such that the outer portion of the implant is dense and in the internal porous. This type of implant provides good shock absorbing capacity with reducing the surface hardness of the implant in addition to reducing the overall weight of the implant. It may be noted that the actual human bone is fact of similar nature. However, limitations in manufacturing technology meant only monolithic objects where possible. The manufacture of gradient objects proposed above possible have been made possible now, thanks to advances in RP.

The stresses are to be found out at the contact regions of the femoral component, UHMWPE tibial component and inside the new implant model between the dense section and porous section. New material Titanium-β alloy is introduced in knee implants, which is having young's modulus nearer to human bone young's modulus. By using this material the stress shielding effect between the knee joint and bone reduces, which reduce bone resorption. The contact stresses are measured at the contact region of femoral and tibial UHMWPE component. The anatomical data is obtained from the CT/MRI scans of patient. MIMICS software is used to build 3D anatomical. The CAD model of the knee is developed using Unigraphics software. Finite element method is used to find the stresses in the knee implant.

Chapter 2

Literature Survey

Oateo arthritis, Rheumatiod arthritis, and Traumatic arthritis are the diseases cause failure of the knee joint. The failure joint is replaced by the artificial components called as knee joint replacement. Rapid Prototyping technology is emerging technology to fabricate the bio-medical implants. The performance of knee joint replacement components are evaluated by experiment and finite element analysis. Nagarjan et al. [10] studied different rapid prototyping technologies used in medical applications. RP technology is useful for fabricating prototypes of complex structures which are suitable to plan complex surgical operations. This procedure used to make physical models without the necessity of specialized tools or fixtures.

Gibson et al. [11] did some case studies on the applications of RP technology in medicine. This technology is applicable in Oral and Maxillofacial surgery, fabricating oral parts and planning proper surgical procedures.

The RP technology is used to study the anatomical structures of human body. The fabricated parts are used for demonstration purpose, teaching in the medical institutions, explaining surgical procedure to patients, etc. By this process the surgical risk and time will be reduced. The process also eases the cost incurred to patient and doctor. [12] [13] [14].

Jeng-Nan lee et al. [15] studied the application of Rapid Prototyping technology and multi axis machining for fabrication of femoral component of the knee prosthesis. The femoral component of the knee joint is designed and manufactured by CAD-CAM process. 3D CAD model is generated from the CT/MRI scans of the patient. The generated data is exported to RP machine (FDM) to fabricate the model. This model is kept as a reference to fabricate the model through multi-axis NC machining process.

Juan Felipe et al. [16] designed and manufactured a skull implant by Titanium alloy. The patient data is acquired by CT/MRI scans and the data is processed to build 3D model of skull. The skull implant is fabricated using Rapid prototyping machine using fused deposition modeling (FDM) machine for validation purpose further Titanium implant is fabricated. The prosthesis was successfully implanted. The results indicates, surgical time was reduced to 85%.

Kruth et al. [17] studied selective laser sintering process in dental prosthesis application. The biocompatible framework of teeth is manufactured by SLS process. The types of materials used are Stainless steel, Titanium alloy, and Cobalt Chromium alloy.

V.K Balla et al. [8] fabricated functional gradient Ti-TiO_2 structures using Laser Engineered Net Shaping (LENS). The structure is made dense on one side and porous on the other side for total hip prosthesis.

Amit et al. [18] studied on the application of Laser Engineered Net Shaping (LENS) to manufacture porous and functionally graded structures for load bearing implants. These type of models will reduce the stress shielding effect and better interaction with bone and the implant.

S.Surya et al. [9] studied on Hybrid manufacturing to fabricate the models. It is an arc-welding based rapid manufacturing process.

Milan et al. [1] studied on the production of medical implants by using rapid prototyping technology and investment casting technology. The anatomical CAD models are developed from the CT/MRI scans of the patient. These CAD models are verified and the data file is exported to the RP machine to fabricate the model. RP and casting methods are used to fabricate the models. ABS material is used to fabricate the prototype of the knee implant. After further verification, the prototype is used to prepare a silicon mold. The metallic implant is fabricated by investment casting process

a) Femoral model using FDM b) Silicon mould c) Fabricated by casting

Figure 2.1: Manufacturing process of Femoral component of knee joint [1]

Tomaso et al. [19] studied effect of contact stress and fatigue life in a knee prosthesis. The contact stresses of knee prosthetic depend on the amount of load applied and the contact area between the femoral and tibial components. It also depends on the angle of flexion and extension. They found that the amount of contact stress is more at the higher flexion angles. The higher contact stresses lead to wear of knee prosthetic. The fatigue life of knee prosthetic depends on the load acting on the knee prosthetic. If the load on the knee prosthetic increases the life of the knee prosthetic decreases.

Pena et al. [20] studied the effect of meniscul tears and meniscectomies on human knee joint by Finite element analysis. The meniscus in the knee joint is multifunctional component; it plays a major role in load transmission, shock absorption and lubrication. The failure of meniscus is the meniscal tear, it causes severe pain in the knee joint. Pena et al conducted FEA analysis on knee joint in three different cases, such as a healthy joint, knee joint with meniscul tear and joint after meniscectomy. The contact stresses are high in the articular cartilage after meniscectomy as compared to that of a knee joint.

Habiba et al. [21] studied the effect of stress shielding in the knee joint after total knee anthroplasty. Failure knee joint is replaced by metallic implants. After knee surgery, the stress shielding increases at the knee joint leading to gradual bone loss and knee joint failure. Habiba et al developed a hybrid implant and conventional implant. The hybrid implant is made of CF/PA-12 femoral lined component with a commercial implant (316L Stainless steel). FEA analysis is done to obtain the stresses at the knee joint between the femoral bone and the implant. In the hybrid implant the stresses produced are less when compared to commercial implant, providing better stress shielding as compared to the conventional implant. The stresses are 63% less compared to conventional implant.

Sivasankar et al. [22] studied the failure analysis of knee prosthesis. Total knee replacement failure is due to loosening of femoral component, tibial-femoral instability, and fatigue failure of tibial tray. These are due to over weight of the body and malallignment of the knee joint. The dynamic and finite element models of fixed and mobile implants are developed and demonstrated the performance of knee joint and contact pressure distribution in the tibio-femoral contact surfaces at different orientations. The contact pressures are less in mobile implants compared to fixed implants at different orientations of the knee joint. The results indicate that the stresses and strains in the distal femur increased with increase in body weight. Malallignment indicate severe stress shielding in the knee joint leads to bone resorption. This will result in more chance to failure of knee joint, induces more pain to the patient.

Bernardo et al. [23] studied the effect of stress shielding in patello-femoral arthroplasty. Surgical repair of patella-femoral joint is known as Patella-femoral arthroplasty where the patella and femoral parts are replaced by artificial components. In this study, the authors developed four finite element models of patello-femoral replacement designs. The implant designs are Richards type II patello-femoral prosthesis, Physiological model of knee, Journey patello-femoral joint prosthesis, and the Genesis II total knee prosthesis. The von misses stresses are evaluated during 120^0 flexion of knee joint and the effect of stress shielding is found. The FEA results are compared with the experimental results. From the results it indicates that during flexion, the Richards II patello-femoral prosthesis has higher stress compared with the other patella-femoral prosthesis, and in Genisis II total knee prosthesis the stress shielding is high compared to physiological model of knee joint.

Kalyana et al. [24] studied on modeling and analysis of a prosthetic knee joint using alternate materials. The materials used in knee replacement surgery must be bio-compatible, light weight and should have high strength to weight ratio. Most commonly used materials in knee replacement surgery are titanium alloys, cobolt chromium alloys, steel alloy, etc. These materials are having high strength but more weight. Chakraverthy et al. considered steel, aluminium, magnesium, glass, boron, UHMWPE, and nano composite material as alternate materials for knee implants. But bio-compatibility of nano materials is to be established. The results indicate that silica reinforced polymer nano composite and UHMWPE gives maximum stresses occur at the low values compared to other materials.

Niinomi et al. [25] studied on preventing stress shielding between the implant and the bone. Stress shielding causes bone resorption and leads to failure of total knee replacement surgery. The patient experiences more pain than before surgery. The implant young's modulus and bone young's modulus is different which increases effect of stress shielding. To reduce the stress shielding between the bone and the implant, alternate materials are introduced which are having low young's modulus and high strength. Titanium-β alloy is a suitable bio-compatible material with low young's modulus. The strength of the alloy is increased, maintaining low young's modulus by various strengthening mechanisms such as work hardening, grain refinement strengthening, etc. The effect of stress shielding is observed in rabbits with Titanium-β alloy, Ti-6Al-4V alloy and Stainless steel 316L. The results indicates, reduction in stress shielding effect in using Titanium-β alloy.

B.R Levine et al [26] studied on clinical performance of porous tantalum in orthopedic surgery which is having a young's modulus of 3 Gpa having high volumetric porosity of 70-80% and excellent biocompatibility.

Lucy et al. [27] studied on wear of total knee replacement. Wear of TKR is due to more contact area and high contact stresses in the knee joint. Wear analysis is performed experimentally and numerically and compared the results. The results show very near values. Author predicted that it taken 2 months to conduct experiment and 2 hours to find computational wear.

Shashishekar et al. [28] studied the effect of sagittal radius, flexion angles and external load on stress in the knee joint. The results indicate, the contact stresses are depend on the sagittal radius of knee joint and lower contact stresses are seen in polyethylene chopped fiber composite artificial joint compared to polyethylene.

Louis et al. [29] studied the motion of the tibiofemoral contact points during in-vivo weight bearing flexion using MRI- based 3D knee models and two orthogonal fluoroscopic images.

Chapter 3

Total Knee Joint Replacement

3.1 Anatomy of knee joint

The knee is a joint that has three compartments, the thigh bone (the femur) meets the large shin bone (the tibia) to form the main knee joint. This joint has an inner (medial) and an outer (lateral) compartment. The kneecap (patella) joins the femur to form a third compartment called the patella-femoral joint. The patella protects the front of the knee joint. The anatomy of knee joint is shown in the Figure 3.1.

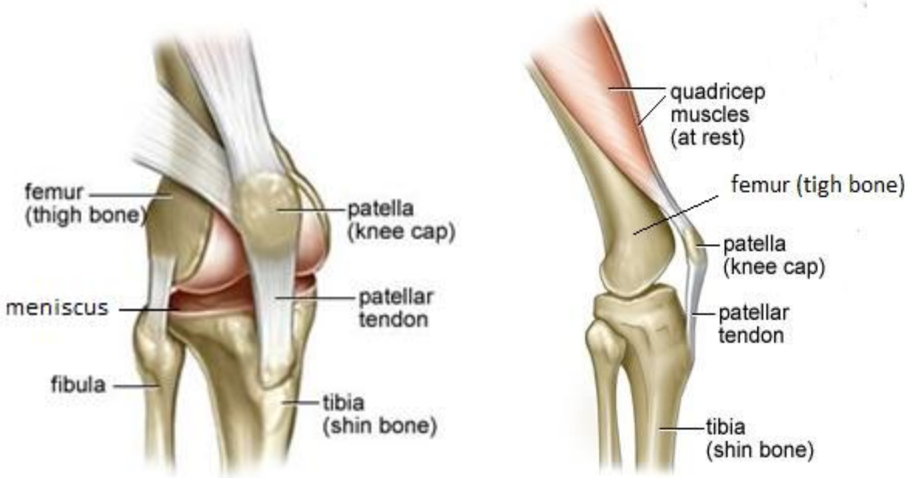

Figure 3.1: Anatomy of Knee Joint [31]

The meniscus is a thickened cartilage pad between the two joints formed by the femur and tibia. The meniscus acts as a smooth surface for motion and absorbs the load of the body above the knee when standing. The knee joint is surrounded by fluid-filled sacs called bursae, which serve as gliding surfaces that reduce friction of the tendons. Below the kneecap, there is a large tendon (patellar tendon) which attaches to the front of the tibia bone. There are large blood vessels passing through the area behind the knee (referred to as the popliteal space). The large muscles of the thigh move the knee. In the front of the thigh, the quadriceps muscles extend the knee joint. In the back of the thigh, the hamstring muscles flex the knee. The knee also rotates slightly under guidance of specific muscles of the thigh. The knee functions to allow movement of the leg and is critical to normal walking. The knee flexes normally to a maximum of 135 degrees and extends to 0 degrees. The bursae, or fluid-filled sacs, serve as gliding surfaces for the tendons to reduce the force of friction as these tendons move. The knee is a weight-bearing joint. Each meniscus serves to evenly load the surface during weight-bearing and also aids in disbursing joint fluid for joint lubrication [25].

3.1.1 Tibiofemoral joint

The joint in the knee between the tibial and the femoral bones is known as Tibio-femoral joint. In between femur and tibial bone there is a thickened cartilage which acts a smooth surface for motion and absorbs the load of the body above the knee when standing is known as meniscus. The knee joint is surrounded by fluid-filled sacs called bursae, which serve as gliding surfaces that reduce friction of the tendons. The distal end of the femur has a curved articular surface that is shaped somewhat like a horseshoe. The femur and tibia are connected together by lateral and medial collateral ligaments. This joint is protected by patella also called as knee cap.

3.1.2 Patellofemoral joint

The patella femoral joint is where the kneecap (patella) and thigh bone (femur) meet. The underside of the patella sits in a groove within the femur called the patella-femoral groove. Within this groove, the patella moves largely lengthwise, but it has some side-to-side movement and can tilt and rotate as well.

3.1.3 Ligaments

Ligament is the fibrous tissue that connects bones to other bones to form a joint. The stability of the knee joint is achieved by ligaments and strong muscles.

Four ligaments are present in the knee joint shown in Figure 3.2, the medial collateral ligament (MCL), lateral collateral ligament (LCL), anterior cruciate ligament

(ACL), and posterior cruciate ligament (PCL). These ligaments provide strength to the knee joint. The medial collateral ligament is located at the inside of the knee joint. It extends from the medial femoral epicondyle to the tibia. This ligament prevents excessive abduction of the knee. The lateral collateral ligament is located at the outside of the knee joint. It extends from the lateral femoral epicondyle to the head of the fibula. This ligament prevents excessive adduction of the knee. The anterior cruciate ligament extends postero-laterally from the tibia and inserts on the lateral femoral condyle. This ligament prevents excessive posterior movement of the femur on the tibia. The posterior cruciate ligament extends antero-medially from the tibia posterior to the medial femoral condyle. This ligament prevents excessive anterior movement of the femur on the tibia.

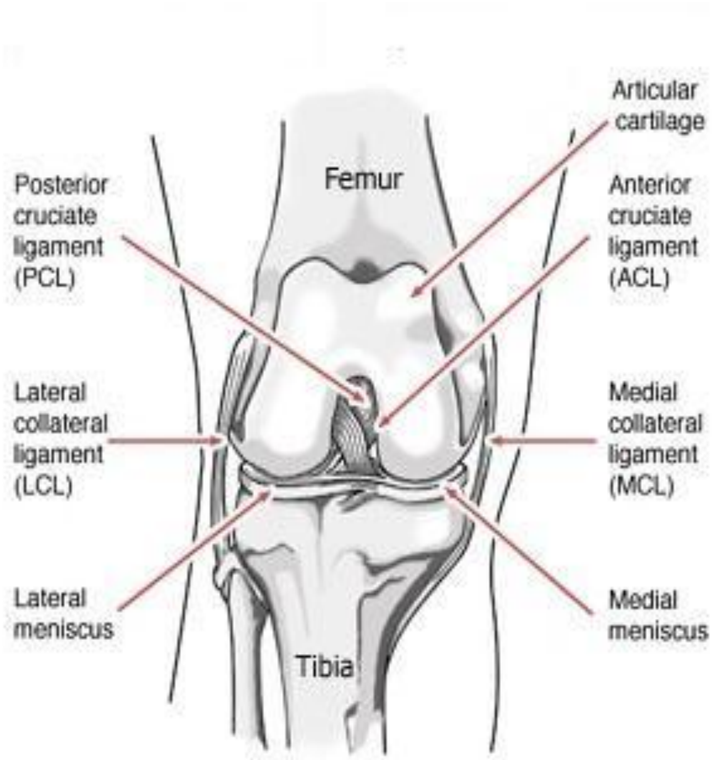

Figure 3.2: Ligament of knee joint

[http://www.daviddarling.info/encyclopedia/L/ligament.html]

3.2 Knee joint motion

3.2.1 Mechanical axis

Mechanical axis refers to the angle formed by a line drawn from the centre of the femoral head to the medial tibial spine and a line drawn from the medial tibial spine and the centre of the ankle joint Figure 3.3. This line is practically perpendicular to the ground.

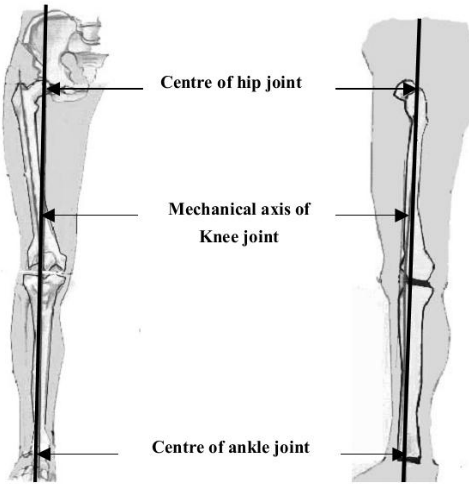

Figure 3.3: Mechanical axis of knee joint

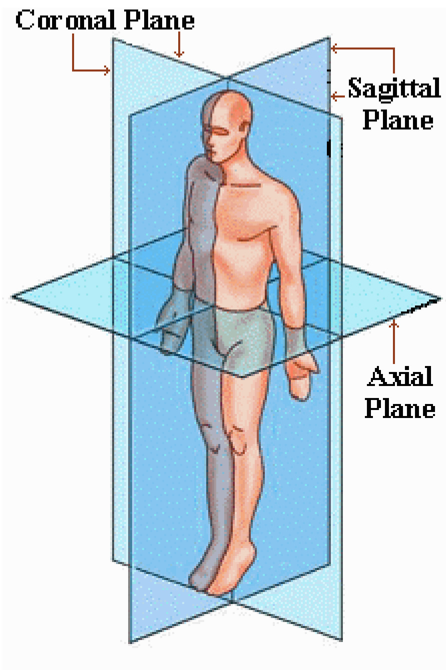

Figure 3.4: Anatomical planes of Human body
[http://www.spineuniverse.com/anatomy/anatomical-planes-body]

3.2.2 Anatomical planes and Axis

Mechanical axis is defined in frontal plane and sagittal plane of human body.
Anatomical planes shown in Figure 3.4 are as follows:

1. ***Sagittal plane*****:** Sagittal plane is a vertical plane which passes from Anterior (front) to Posterior (rear) dividing the body into right and left halves.

2. ***Coronal plane:*** A coronal plane (also known as the frontal plane) is any vertical plane that divides the body into ventral and dorsal (belly and back) sections.

3. ***Transverse plane:*** The transverse plane lies horizontally and divides the body into superior (upper) and inferior (lower) parts.

An axis is a straight line around which an object rotates. Movement at the joint take place in a plane about an axis. There are three axis of rotation. Sagittal axis, Frontal axis and Vertical axis. Knee joint motions are shown in the Figure 3.5 and briefly tabulated in Table 3.1

1. ***Sagittal axis:*** The sagittal axis passes horizontally from posterior to anterior and is formed by the intersection of the sagittal and transverse planes.

2. ***Frontal axis:*** The frontal axis passes horizontally from left to right and is formed by the intersection of the frontal and transverse planes.

3. ***Vertical axis:*** The vertical axis passes vertically from inferior to superior and is formed by the intersection of the sagittal and frontal planes.

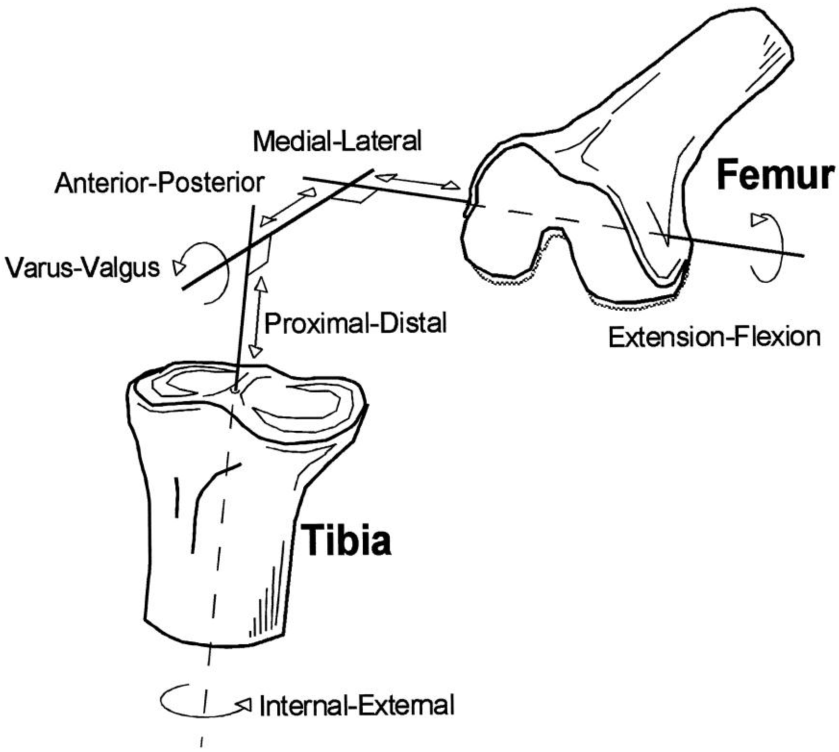

Figure 3.5: Knee joint motions.

[http://ajs.sagepub.com/content/27/4/533/F1.expansion]

The motions of knee joint are briefly tabulated below in Table 3.1

Table 3.1: Planes, axis, motions and examples of knee joint

Plane	Axis	Motion	Example
Sagittal	Frontal	Rotation: Flexion/extension Translation: Medial/Lateral	Walking, squatting.
Coronal	Sagittal	Rotation: Adduction/Abduction Translation: Anterior/Posterior	Side bending.
Transverse	Vertical	Rotation: Axial Translation: Superior/Inferior	Turning either left/right side.

3.3 Structure and mechanical properties of human bone

3.3.1 Structure of bone

Bones are to be strong to support our body weight and in some cases provide protection. It is an anisotropic, heterogeneous and viscoelastic material. Every bone has an outer layer that is dense, solid and smooth. This outer layer covers a sponge like internal layer. There are two types of bone tissue: compact and spongy. The names imply that the two types differ in density, or how tightly the tissue is packed together. There are three types of cells that contribute to bone homeostasis. Osteoblasts are bone-forming cell, osteoclasts resorb or break down bone, and osteocytes are mature bone cells. Equilibrium between osteoblasts and osteoclasts maintains bone tissue.

Compact bone*:* Compact bone consists of closely packed osteons or haversian systems. The osteon consists of a central canal called the osteonic (haversian) canal, which is surrounded by concentric rings (lamellae) of matrix. Between the rings of matrix, the bone cells (osteocytes) are located in spaces called lacunae. Small channels (canaliculi) radiate from the lacunae to the osteonic (haversian) canal to provide passageways through the hard matrix. In compact bone, the haversian systems are packed tightly together to form what appears to be a solid mass. The osteonic canals contain blood vessels that are parallel to the long axis of the bone. These blood vessels interconnect, by way of perforating canals, with vessels on the surface of the bone.

Trabecular bone**:** Filling the interior of the bone is the trabecular bone tissue (an open cell porous network also called cancellous or spongy bone), which is composed of a network of rod- and plate-like elements that make the overall organ lighter and allow room for blood vessels and marrow. Trabecular bone accounts for the remaining 20% of total bone mass but has nearly ten times the surface area of compact bone. Its porosity is 30–90%. If, for any reason, there is an alteration in the strain the cancellous is subjected to, there is a rearrangement of the trabeculae.

The microscopic difference between compact and cancellous bone is that compact bone consists of haversian sites and osteons, while cancellous bones do not. Also, bone surrounds blood in the compact bone, while blood surrounds bone in the cancellous bone.

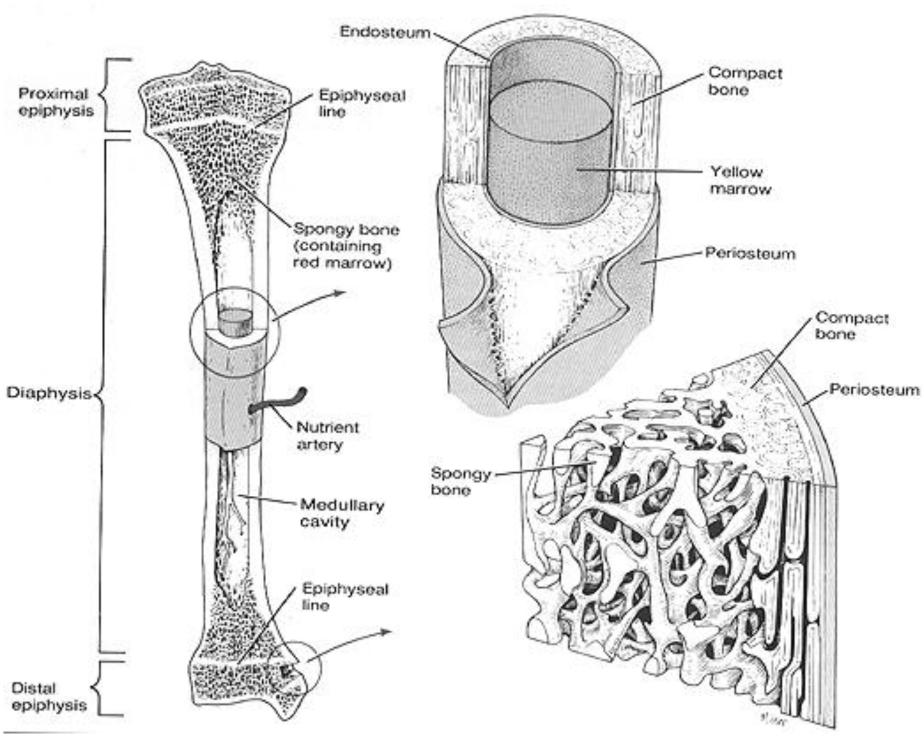

Figure 3.6: Bone structure

[http://www.learn-free-medical-transcription.blogspot.in/2010/06/compact-bone-and-cancellous-bone-lesson.html]

.

3.3.2 Mechanical properties

Human bone is an isentropic, heterogeneous and viscoelastic material which should withstand the weight of the body and to stabilize the body. For this, bones must comprise of good compressive and tensile strength. The average density of bone is around 1500 kg/m^3. The mechanical properties of the bone are tabulated in Table 3.2.

Table 3.2: Mechanical properties of bone [30]

Property	Longitudinal	Transverse
Young's modulus (MPa)	17,000	11,500
Ultimate tensile strength (MPa)	133	51
Ultimate compressive strength (MPa)	193	133
Ultimate strain	3.1%	0.7%

3.4 Total knee replacement

3.4.1 Causes for failure of knee joint

The common causes of knee pain and loss of knee function in clinic are osteoarthritis, rheumatoid arthritis and post traumatic arthritis. Osteoarthritis usually occurs after the age of 50 and often in an individual with a family history of arthritis. The cartilage that cushions the bones of the knee softens and wears away. The bones then rub against one another causing knee pain and stiffness. Rheumatoid arthritis is a disease inwhich the synovial membrane becomes thickened and inflamed, producing too much synovial fluid, which over-fills the joint space. This chronic inflammation can damage the cartilage and eventually cause cartilage loss, pain and stiffness. Rheumatoid arthritis can follow a serious knee injury. A knee fracture or severe tears of the knee's ligaments may damage the articular cartilage over time, causing knee pain and limiting knee function. If the knee joint is severely damaged by arthritis or injury, it may be hard to perform simple activities such as walking or climbing stairs. The patient may begin to feel pain while sitting or lying down. If medication, changing activity level and using walking supports are no longer helpful, total knee replacement surgery will be considered. By resurfacing damaged and worn surfaces of the affected knee joint, total knee replacement surgery can relieve knee pain, correct leg deformity and allow the patient to resume normal activities.

Figure 3.7: Healthy knee joint(Right) and Damaged knee joint(Left)

[http://www.aclsolutions.com/anatomy.php]

3.4.2 Types of knee replacement implants

Total knee replacement implants are not one size fit or one style fit. It may vary by design, fixation and materials. Typical total knee replacement implants have three basic components. They are femoral, tibial and patellar components [32].

Femoral component: This component is generally made of metal. This component is fixed to the end of femur (thigh bone). There is a groove down the centre of this part of the implant which allows the patella or also called as knee cap to move up and down as the knee bends and straightens.

Tibial component: This component is divided into two sub components. One is flat metal platform and another is ultra-high molecular weight polyethylene spacer. UHMWPE is placed over the flat metal surface and it will provide cushioning effect.

Patellar component: This component is made of metal. It is like dome shaped piece. This implant is used in some of the knee replacements.

Figure 3.8: Total knee implant components [32]

3.4.3 Types of implants:

Fixed bearing implants, Mobile bearing implant, Medial pivot implants, Posterior cruciate ligament (PCL) retaining or substituting implant and Cemented and cement-less implant, total knee and partial knee replacement respectively.

Fixed bearing implant: Fixed bearing implant is the most common type of implant in total knee replacement. The implant is termed as fixed because the polyethylene cushion of the tibial component is fixed firmly to the metal platform base.

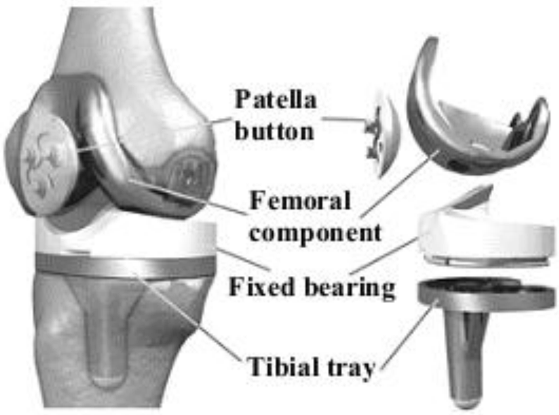

Figure 3.9: Fixed bearing implant [32]

The femoral component slides over the UHMWPE tibial component. This implant provides a good range of motion. The failure of this type of bearing occurs due to excessive activity or additional weight. This wear can cause loosening of the implant, causing pain and joint failure.

Mobile bearing implants: Mobile bearing implant is special type of implant designed for younger, more active and overweight for longer performance with less wear. The term mobile is referred as the polyethylene insert in the tibial component can rotate short distances inside the metal tibial tray. This rotation allows patients a few degrees of greater rotation to the medial and lateral sides of the knee.

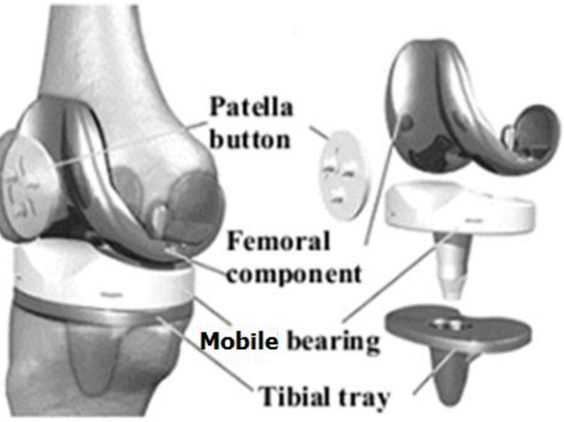

Figure 3.10: Mobile bearing implant [32]

Medial pivot implants: This type of implant more look like a natural knee as it rotates, twists, bends, flexion's and stables. This type of design is more stable during normal knee motion.

Posterior cruciate ligament (PCL) retaining or substituting implant: The posterior cruciate ligament (PCL) is an important structure that stabilizes the knee joint. With some knee replacements, the posterior cruciate ligament is defective and removed, and with others it is left intact. The anterior cruciate ligament is usually removed for a total knee replacement, and left in place for a uni-compartmental replacement. After removal of the PCL, a special total knee prosthesis that simulates the function of the PCL should be implanted. The stabilization of the total knee joint in these prostheses is achieved by a 'cam and post' mechanism added to the prosthesis components. This mechanism replaces the function of the PCL [32].

Figure 3.11: Posterior cruciate ligament (PCL) retaining (right) and substituting implant (left) [32]

Cemented and cement-less implant: This type of implants depends on the type of fixation i.e., cemented, cement-less or hybrid (combination of both) designs. The majority of implants are cemented. In cemented implants for fixation, a special kind of bone cement polymethyl-methacrylate (PMMA) is used to hold the implants in place. PMMA is a polymer that is mixed at the time of implantation. The cementless implants have a roughened or porous surface at the bone/implant interface. Most implant surfaces are textured or coated with a porous material so that the new bone actually grows into the surface of the implant. In some cases screws may also be used to stabilize the implant until the bone ingrowth occurs.

There is another option called hybrid TKR with an uncemented femoral component and cemented tibial and patellar components.

Total knee replacement and Partial knee replacement: Failure knee joint may be repaired either totally or partially replacing the failure components. They are known as total knee replacement and partial knee replacement respectively. Total knee replacement means the total knee joint parts are replaced by artificial components such as femoral, tibial and patellar components. A partial knee replacement is also called as unicompartmental knee replacement. This type of knee joint replacement is performed were one side of femoral or tibial part is damaged [32].

Figure 3.12: Unicompartmental (Right) and Total knee replacement (Left) [32]

Chapter 4

Generation of CAD model of a knee joint implant

4.1 Processing of image data

Failure of knee joint is identified through CT/MRI scans of the patient. The data from CT/MRI scanning typically available in the DICOM (Digital Imaging and Communications in Medicine) format. In this format, the tissue related information is stored in 2D pictures for each layer. The CAD model of the joint can be generated by stacking all these 2D DICOM figures together and stitching them into a 3D model. MIMICS, from materialise, an dedicated BioMedical software has been used to carry out the conversion. The missing part or the counters of the damaged part are also developed in MIMICS software. These counters are exported to CAD software where the implant 3D geometrical model can be created.

The following are the basic steps to obtain a 3D model in medical industry:

1. Data acquisition
2. Data processing
3. Model manufacturing
4. Clinical application

4.1.1 Data acquisition: The detailed anatomical data is acquired by two techniques; Computed Tomography and Magnetic Resonance Imaging scans.

4.1.2 Data processing: The anatomical data acquired is 2D images. From these images, the 3D model should be developed. MIMICS software is used to develop 3D anatomical structures. The following procedure explains the construction of 3D model from CT/MRI scans using MIMICS:

a) Import the CT/MRI scans to MIMICS. All the images will be loaded and displayed in axial, coronal, and sagittal views.
b) Set the grey values to achieve a good collection of pixels of interest that constitutes an object.
c) Set the thresholding values. Low threshold values are used to select the soft tissues and high threshold value is used to select the dense parts.
d) Region growing tool used to split the segmentation created thresholding and to remove the floating pixels.
e) Building of 3D model by calculating the data at the new region of interest, it develops the 3D anatomical model.

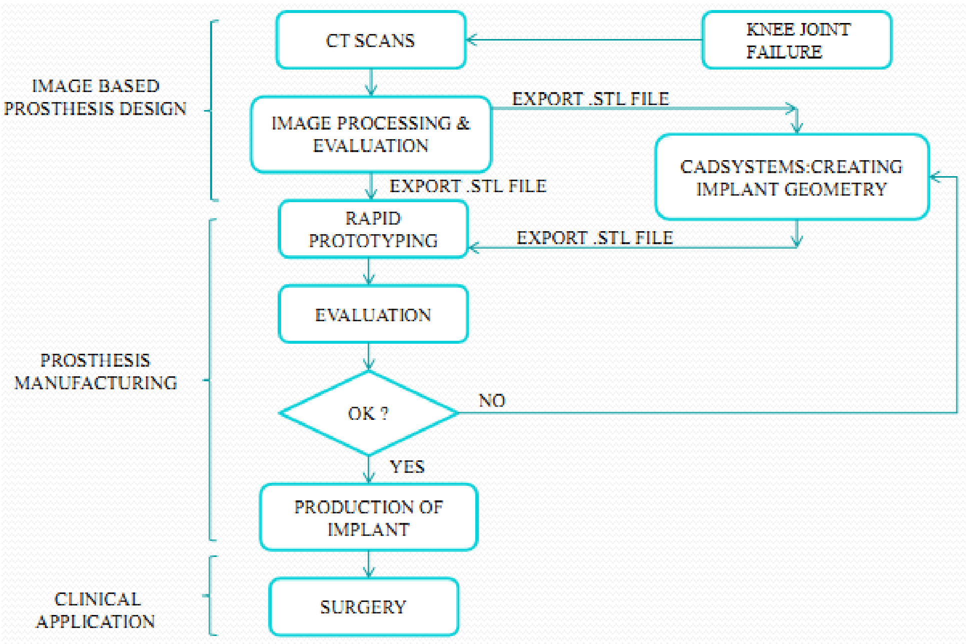

Figure 4.1: Flow chart diagram on processing of scanned data – clinical application

4.1.3 Model Manufacturing: Rapid prototyping is emerging technology in the field of medicine to fabricate 3D anatomical models. Many researchers used various RP processes to manufacture the anatomical models as discussed in literature survey.

4.1.4 Clinical application: The manufactured prosthesis or implants are used in replacing the failure parts in the body.

Figure 4.2 shows the 3D anatomical data of human knee joint femoral part, which is acquired from the CT scan data, processed through MIMICS 14.12 software.

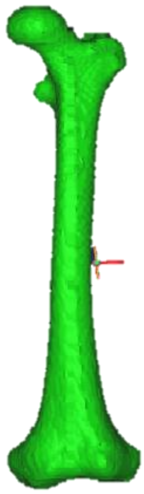

Figure 4.2: Femur (Thigh bone)

4.2 CAD model of knee joint implant:

3D geometrical model of knee joint implant is designed using Unigraphics NX7.5 software. The dimensions of femoral component are taken from the femur bone. The geometrical model of femoral component, tibial components is shown in the Figure 4.3.

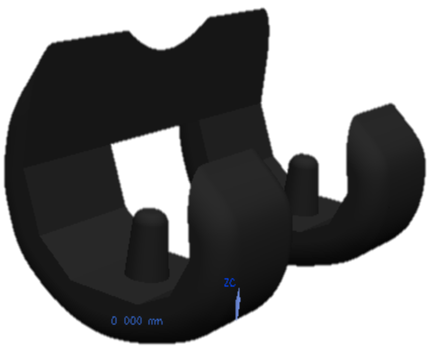

a) Femoral component

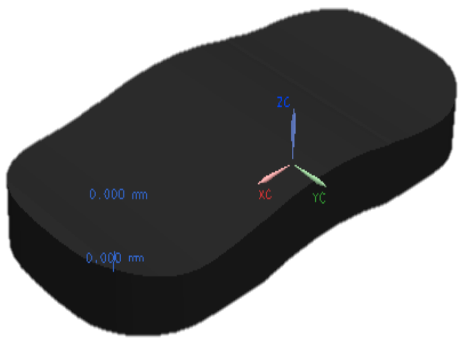

b) Tibial UHMWPE component

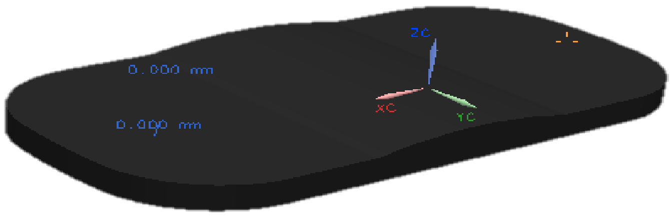

c) Tibial baseplate component

Figure 4.3: Components of knee joint implant

The dimensions of knee implant components are shown in the table 4.1:

Table 4.1: Dimensions of knee joint implants

Dimension (mm)	Femoral component	Tibial UHMWPE component	Tibial baseplate
Length	89	84	84
Width	54	45	45
Height	45	8	6

In the present research work, a new femoral implant model is designed which suits the need of the doctors and patients. The model is designed as dense section at the outside compartment and porous section at the inside compartment. Advantage of this model is, it reduces weight of the component which is beneficial factor for patient. The implant is shown in the Figure 4.4.

Figure 4.4: Improved femoral implant

The assembly of knee joint implant consists of femoral component, tibial UHMWPE component and tibial baseplate are shown in the Figure

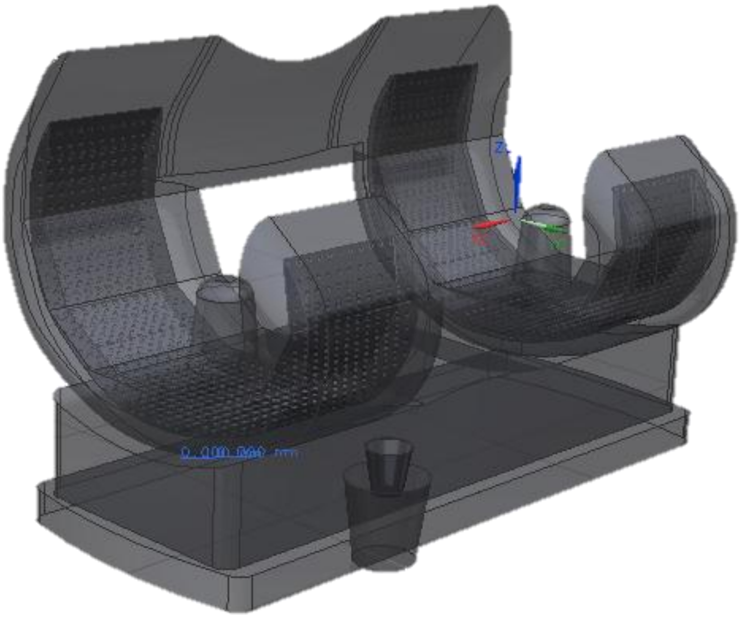

Figure 4.5: Assembly of improved knee implant

During the knee motion, the knee flexion's and extends from 0^0 to 90^0 shown in the Figure.

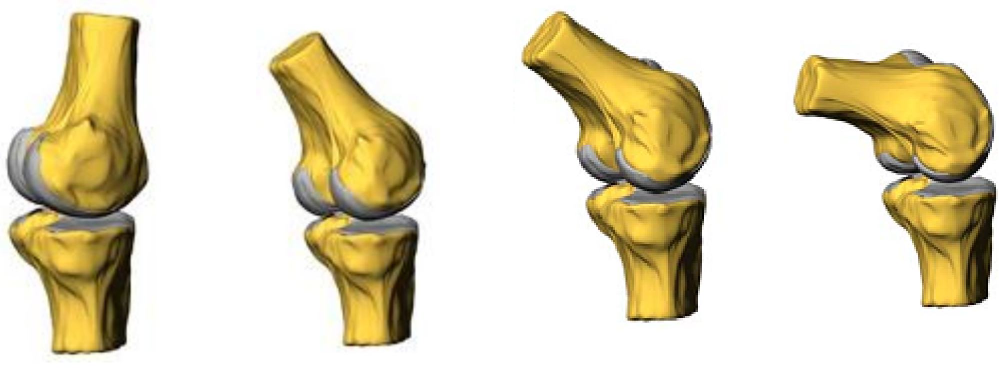

a) 0-degrees b) 30-degrees c) 60-degrees d) 90-degrees

Figure 4.6: Knee motion from 0^0 to 90^0 [29]

Considering the knee joint kinematics, various geometric orientations of the knee joint implant are modelled shown in the Figure 4.7.

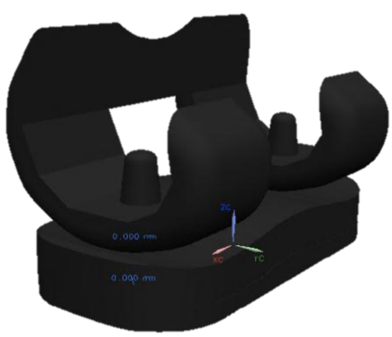

a) Zero degree

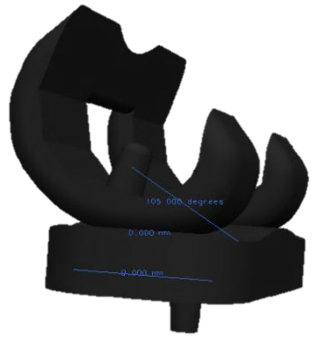

b) 15 degree

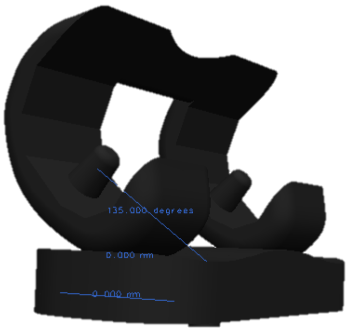

c) 45 degree

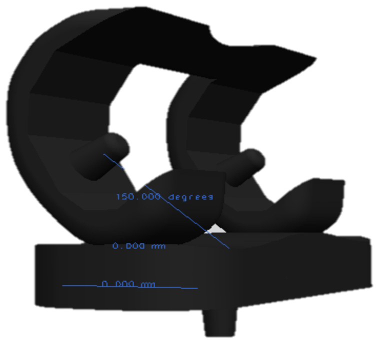

d) 60 degree

Figure 4.7: Various orientations of knee joint implant

These models have been used in the subsequent chapters for analysis.

Chapter 5

Static analysis of total knee replacement

Static analysis of knee joint implant is done by using FEM in ANSYS-WORKBENCH environment.

5.1 Governing equations:

The basic governing equation for the given problem is

$$EA\frac{d^2u}{dz^2} + q = 0 \tag{5.1}$$

where the Boundary conditions are:

$$\text{at } z = 0\,;\, u(0) = 0$$

$$\text{at } z = l\,;\, EA\frac{du}{dz} = -F$$

Equilibrium equations are:

$$\frac{\partial \sigma_x}{\partial x} + \frac{\partial \tau_{xy}}{\partial y} + \frac{\partial \tau_{xz}}{\partial z} + f_x = 0 \tag{5.2}$$

$$\frac{\partial \tau_{xy}}{\partial x} + \frac{\partial \sigma_y}{\partial y} + \frac{\partial \tau_{yz}}{\partial z} + f_y = 0 \tag{5.3}$$

$$\frac{\partial \tau_{xz}}{\partial x} + \frac{\partial \tau_{yz}}{\partial y} + \frac{\partial \sigma_z}{\partial z} + f_z = 0 \tag{5.4}$$

The constitutive equation:

$$\{\sigma\} = [D]\{\epsilon\} \tag{5.5}$$

where

$$\{\sigma\} = \left\{\sigma_x \;\; \sigma_y \;\; \sigma_z \;\; \tau_{xy} \;\; \tau_{yz} \; \tau_{xz} \right\}^T \tag{5.6}$$

$$\{\in\} = \left\{\in_x \;\; \in_y \;\; \in_z \;\;\; \gamma_{xy} \;\; \gamma_{yz} \, \gamma_{xz} \right\}^T \tag{5.7}$$

Equations for small displacements:

$$\begin{Bmatrix} \in_x \\ \in_y \\ \in_z \\ \gamma_x \\ \gamma_x \\ \gamma_x \end{Bmatrix} = \begin{Bmatrix} \frac{\partial u}{\partial x} \\ \frac{\partial y}{\partial y} \\ \frac{\partial w}{\partial z} \\ \frac{\partial u}{\partial y} + \frac{\partial v}{\partial x} \\ \frac{\partial v}{\partial z} + \frac{\partial w}{\partial y} \\ \frac{\partial u}{\partial z} + \frac{\partial w}{\partial x} \end{Bmatrix} \tag{5.9}$$

Traction boundary condition:

$$\varphi_x = \sigma_x n_x + \tau_{xy} n_y + \tau_{xz} n_z = \bar{\varphi}_x \tag{5.10}$$

$$\varphi_y = \tau_{xy} n_x + \sigma_y n_y + \tau_{yz} n_z = \bar{\varphi}_y \tag{5.11}$$

$$\varphi_z = \tau_{xz} n_x + \tau_{yz} n_y + \sigma_z n_z = \bar{\varphi}_z \tag{5.12}$$

Element stiffness matrix for tetrahedron element

Let us assume a linear function:

$$u = [1\ x\ y\ z\ ] \begin{Bmatrix} a_1 \\ a_2 \\ a_3 \\ a_4 \end{Bmatrix} = [X]\{A\} \tag{5.13}$$

Evaluation of *u* at every node:

$$\{u\} = [\bar{X}]\{A\} \tag{5.14}$$

$$[\bar{X}] = \begin{bmatrix} 1 & x_1 & y_1 & z_1 \\ 1 & x_2 & y_2 & z_2 \\ 1 & x_3 & y_3 & z_3 \\ 1 & x_4 & y_4 & z_4 \end{bmatrix} \tag{5.15}$$

Inverse of matrix $[\bar{X}]$ in Eq. and substitution of the resulting expression into Eq. gives

$$u = [X][\bar{X}]^{-1}\{u\} = [H]\{u\} \tag{5.16}$$

Where the shape functions are:

$$[H] = [H_1(x,y,z) \quad H_2(x,y,z) \quad H_3(x,y,z) \quad H_4(x,y,z)] \tag{5.17}$$

we use the same shape functions for the three displacements

$$\begin{Bmatrix} u \\ v \\ w \end{Bmatrix} = \begin{bmatrix} H_1 & 0 & 0 & H_2 & 0 & 0 & H_3 & 0 & 0 & H_4 & 0 & 0 \\ 0 & H_1 & 0 & 0 & H_2 & 0 & 0 & H_3 & 0 & 0 & H_4 & 0 \\ 0 & 0 & H_1 & 0 & 0 & H_2 & 0 & 0 & H_3 & 0 & 0 & H_4 \end{bmatrix} \begin{Bmatrix} u_1 \\ v_1 \\ w_1 \\ u_2 \\ v_2 \\ w_2 \\ u_3 \\ v_3 \\ w_3 \\ u_4 \\ v_4 \\ w_4 \end{Bmatrix}$$

$$= [N]\{d\} \tag{5.18}$$

where $\{d\}$ is the nodal displacement vector.

$$\{\in\} = [B]\{d\} \tag{5.19}$$

in which

$$[B]=\begin{bmatrix} \frac{\partial H_1}{\partial y} & \frac{\partial H_1}{\partial x} & 0 & \frac{\partial H_2}{\partial x} & 0 & 0 & \frac{\partial H_3}{\partial x} & 0 & 0 & \frac{\partial H_4}{\partial x} & 0 & 0 \\ 0 & \frac{\partial H_1}{\partial z} & \frac{\partial H_1}{\partial y} & 0 & \frac{\partial H_2}{\partial x} & 0 & 0 & \frac{\partial H_1}{\partial x} & 0 & 0 & \frac{\partial H_4}{\partial y} & 0 \\ \frac{\partial H_1}{\partial z} & 0 & \frac{\partial H_1}{\partial x} & 0 & 0 & \frac{\partial H_2}{\partial x} & 0 & 0 & \frac{\partial H_3}{\partial x} & 0 & 0 & \frac{\partial H_4}{\partial z} \\ \frac{\partial H_1}{\partial y} & \frac{\partial H_1}{\partial x} & 0 & \frac{\partial H_2}{\partial y} & \frac{\partial H_2}{\partial x} & 0 & \frac{\partial H_3}{\partial x} & \frac{\partial H_3}{\partial x} & 0 & \frac{\partial H_4}{\partial y} & \frac{\partial H_4}{\partial x} & 0 \\ 0 & \frac{\partial H_1}{\partial z} & \frac{\partial H_1}{\partial y} & 0 & \frac{\partial H_1}{\partial z} & \frac{\partial H_2}{\partial y} & 0 & \frac{\partial H_1}{\partial z} & \frac{\partial H_3}{\partial y} & 0 & \frac{\partial H_4}{\partial z} & \frac{\partial H_4}{\partial y} \\ \frac{\partial H_1}{\partial z} & 0 & \frac{\partial H_1}{\partial x} & \frac{\partial H_2}{\partial z} & 0 & \frac{\partial H_2}{\partial x} & \frac{\partial H_3}{\partial z} & 0 & \frac{\partial H_3}{\partial x} & \frac{\partial H_1}{\partial z} & 0 & \frac{\partial H_4}{\partial x} \end{bmatrix} \tag{5.20}$$

5.2 Assumptions in the model:

The following assumptions are made in solving the problem numerically

1. The knee implant is made of linear, elastic, isotropic, homogeneous material.
2. The contact surfaces are perfectly bonded together.
3. The vertical load applied on femoral component.
4. The tibial tray is fixed and constrained in all degrees of freedom.
5. In the mobile bearing implants, polyethylene insert is made to rotate with movement of femoral component.
6. In the fixed implants, polyethylene insert is fixed to the tibial tray, and there is no movement with the femoral component.

5.3 Mesh development:

The knee joint model is meshed with h-adaptive technique, using TET10 element, shown in the Figure 5.1 and Figure 5.2 for Model 1(solid) and Model 2(Dense outside & Porous inside) respectively.

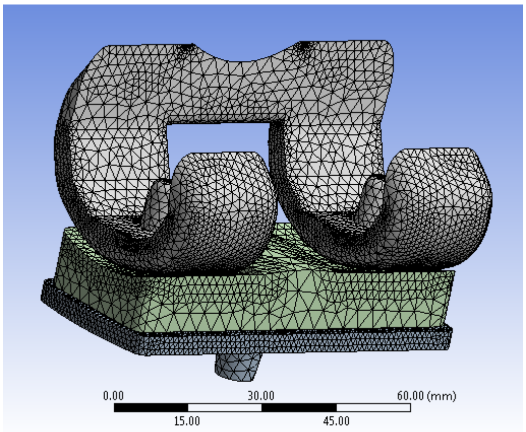

a) Zero Degrees

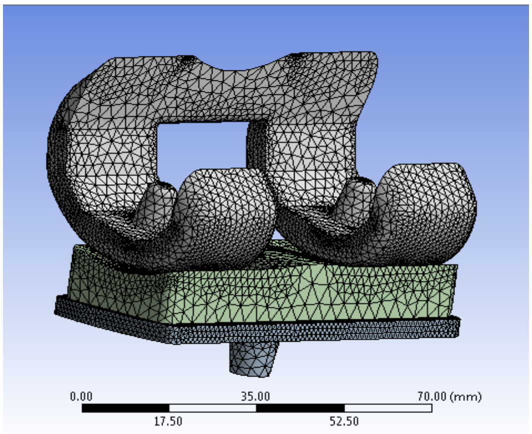

b) 15 Degrees

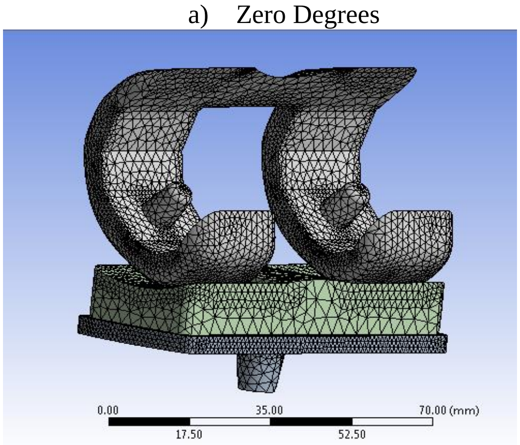

c) 45 Degrees

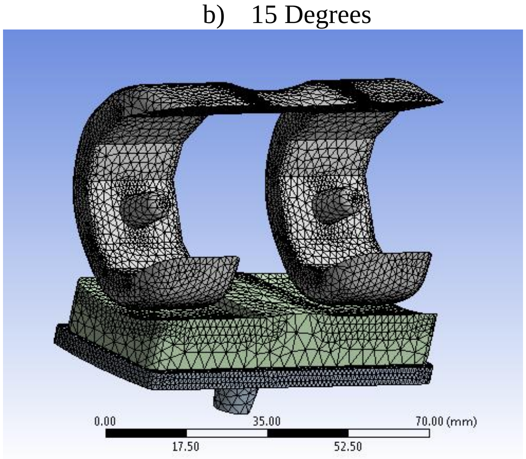

d) 60 Degrees

Figure 5.1: Mesh of Model 1knee joint implants

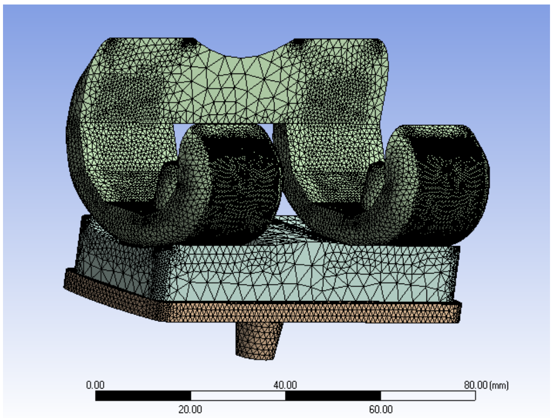

a) Zero Degrees

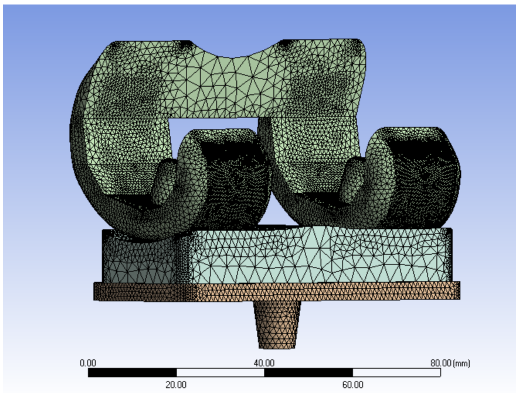

b) 15 Degrees

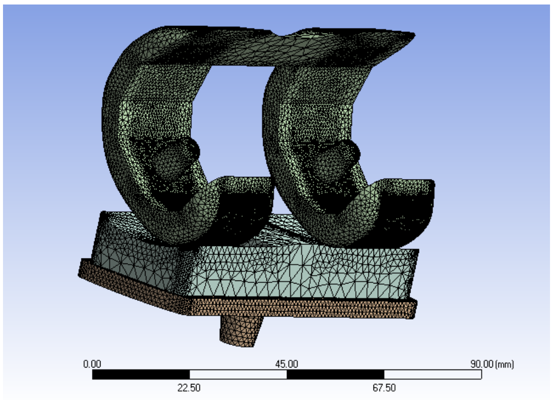

c) 45 Degrees

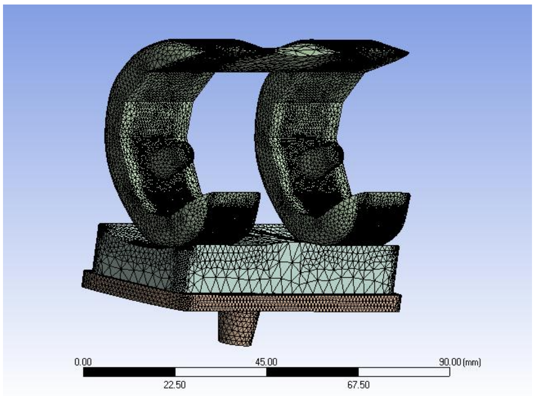

d) 60 Degrees

Figure 5.2: Mesh of Model 2 knee joint implants

Mesh size

A mesh size of 5mm is used and mesh refinement is made at the contact regions of Femoral, PE Insert and Tibial components respectively. The mesh details for knee joint implant are tabulated in Table 5.1

Table 5.1: Mesh details

	Model 1		Model 2	
Flexion angle(^{0})	Nodes	Elements	Nodes	Elements
0	478044	318822	1377134	924946
15	477950	318736	1376018	924068
45	474816	317222	1378258	925750
60	476780	317895	1375546	923715

5.4 Materials and their properties:

Materials: The materials used in knee joint replacement surgery must have certain properties like:

- Biocompatibility,
- Non-corrosive,
- Non-toxic and
- Anti-allergic.

The following are some materials which used in knee joint implants by researchers and medical practioners:

1. Cobalt chromium alloy (CoCrMo)
2. Titanium alloy’s
    i. Ti-6Al-4V
    ii. Ti-29Nb-13Ta-4.6Zr also known as TNTZ etc.
3. Stainless steel 316L
4. Ultra High Molecular Weight Polyethylene (UHMWPE)
5. Porous Tantalum

Properties:

The properties of materials are tabulated in Table 5.2

Table 5.2: Mechanical properties of materials

Material	Density (Kg/m3)	Youngs modulus(Gpa)	Poissons ratio	Tensile yield strength(Mpa)	Ultimate tensile strength (Mpa)
CoCr	7990	200	0.3	560	1000
Ti6Al4V	4430	113.8	0.36	880	950
TNTZ	6075	50	0.36	800	820
SS 316L	7990	193	0.3	290	558
UHMWPE	926	0.69	0.45	21	48
Tantalum	16650	3.5	0.34	51	110

5.5 Model validation:

The failure of knee joint replacement is because of wear between the knee joint components (Femoral component, PE insert and Tibial Tray). The early detection of contact stresses in the components prevents wear and increases the life of knee joint replacement. Tomaso et, al [18] conducted experiments on knee joint component to find the contact stresses at different stages of gait cycle in between Femorel component, Tibial Tray and PE insert. The femoral component and Tibial Tray is made of Cobalt chromium and bearing component is made of Ultra High Molecular Weight Polyethylene. The CAD model of knee joint components is validated by the experimental results. Vertical load is applied on the model at various flexion angles from $15^0 – 60^0$ as follows:

Flexion angle (^{0})	Load applied (N)
15	2200
45	3200
60	2800

The maximum pressure is calculated at the contact regions between Femoral component, PE insert, and Tibial Tray tabulated in Table 5.3

Table 5.3: Validation of Results

Superior surface

Flexion angle (^{0})	Load applied (N)	Experiment (MPa)	FEM (MPa)
15	2200	14.5	7.46
45	3200	27.7	30.5
60	2800	24.5	20.15

Interior surface

Flexion angle (^{0})	Load applied (N)	Experiment (MPa)	FEM (MPa)
15	2200	6.5	3.7
45	3200	11.5	9.1
60	2800	9.5	7.3

Figure 5.3 shows model validation for maximum pressures at the contact regions of knee implant between Experimental results and FEM simulations.

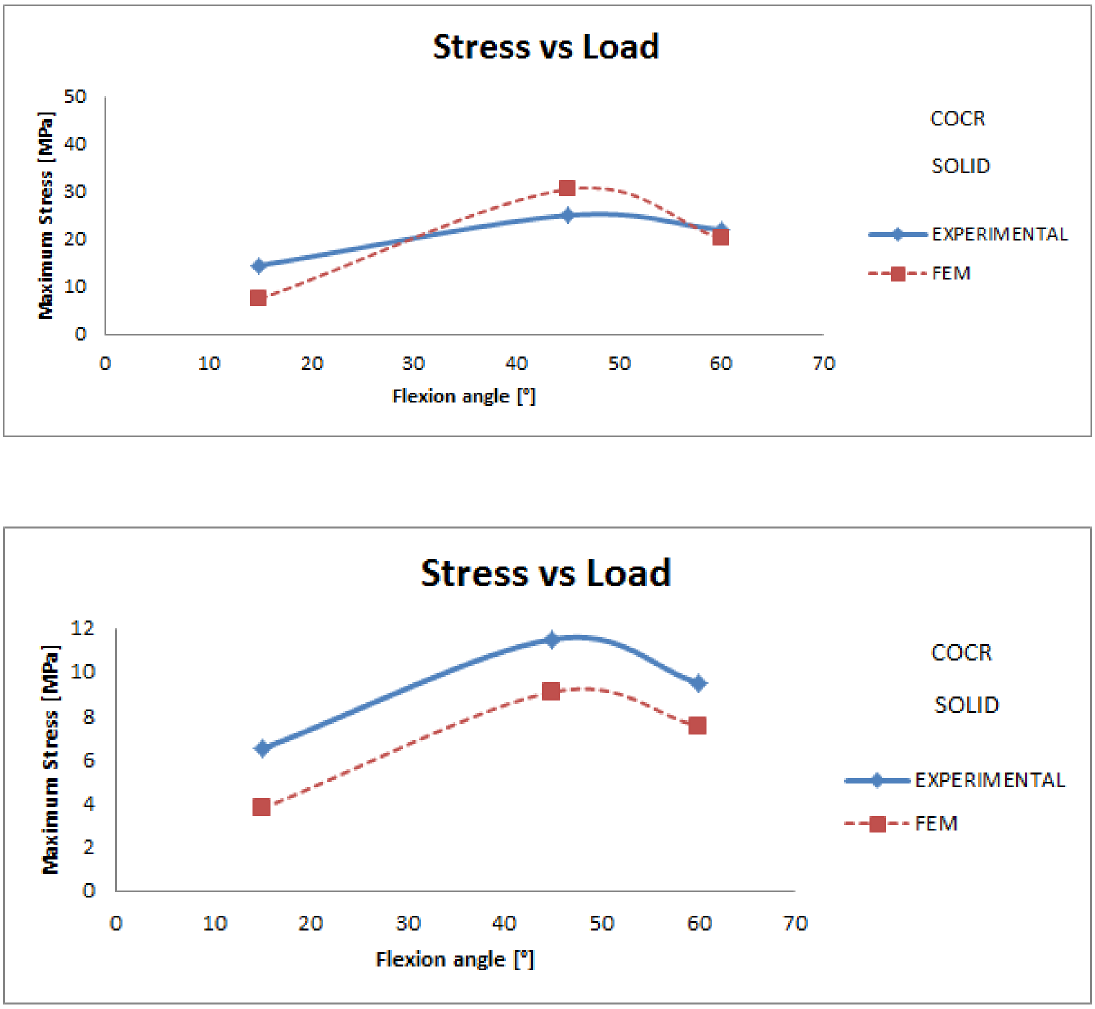

Figure 5.3: Validation of FEM simulations with Experiment results

From the model validation results, the FEM simulations are conducted on the knee joint implant using different materials on proposed new knee joint implant made of dense material outside and porous material inside and are discussed in the following chapters.

Chapter 6
Results and Discussion

The new knee joint implant is made of two different materials, to reduce the overall weight of implant. Finite Element Analysis is performed on the new improved knee joint implant, to determine the contact stresses between Femoral component & PE insert and the stress shielding effect in between the bone and the Femoral component. In this process, two cases were studied.

Case 1: Titanium alloy (Ti-6Al-4V) is used outside and Porous tantalum is used inside the body.

Case 2: Titanium β-alloy (TNTZ) is used outside and Porous Tantalum is used inside the body.

The contact stresses between Femoral component and PE insert for above two cases are obtained at different flexion angles and are compared with the experimental results [18] and tabulated in Table 6.1. From the results it is found that, the contact stresses are less compared to the experimental results. This proves that the improved knee joint model is best and increases life of the knee joint implant. The stresses on the Femoral component are considered from the FEM validation results and are compared with the new improved knee joint models made of Ti6Al4V + Ta and TNTZ + Ta, it is found that the stresses on Femoral component are less. This indicates reduction in stress shielding effect and bone resorption between the implant and the bone. The results are tabulated in Table 6.2.

Table 6.1: Contact stresses between FC and PE insert Experiment and FEM

Flexion angle (⁰)	Load applied (N)	Experimental Stress (MPa)	Stress (Ti6Al4V+Ta) (MPa)	Stress (TNTZ+Ta) (MPa)
15	2200	14.5	6.39	6.75
45	3200	27.7	42.44	42.82
60	2800	24.5	16.9	17.32

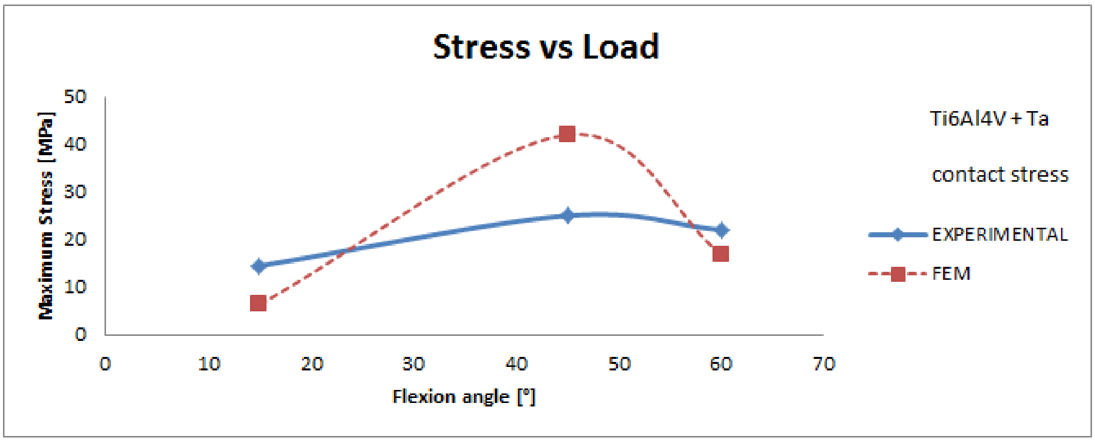

a) Ti6Al4V + Ta

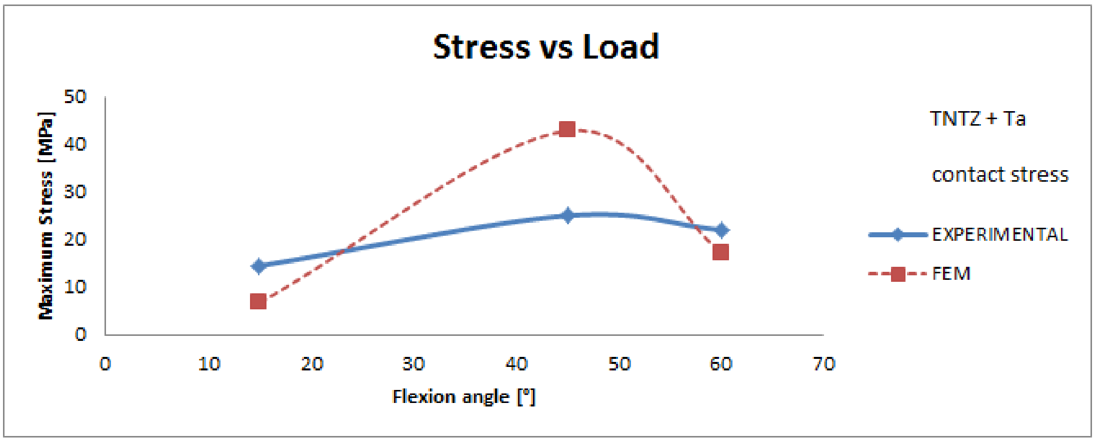

b) Ti6Al4V + Ta

Figure 6.1: Comparison of contact stresses between FC and PE insert for Experiment and FEM

Table 6.2: Contact stresses on the Femoral component

Flexion angle (^{0})	Load applied (N)	Stress (CoCr) (MPa)	Stress (Ti6Al4V+Ta) (MPa)	Stress (TNTZ+Ta) (MPa)
15	2200	37.16	48.75	45.54
45	3200	128.27	101.73	93.45
60	2800	100.48	110.65	101.49

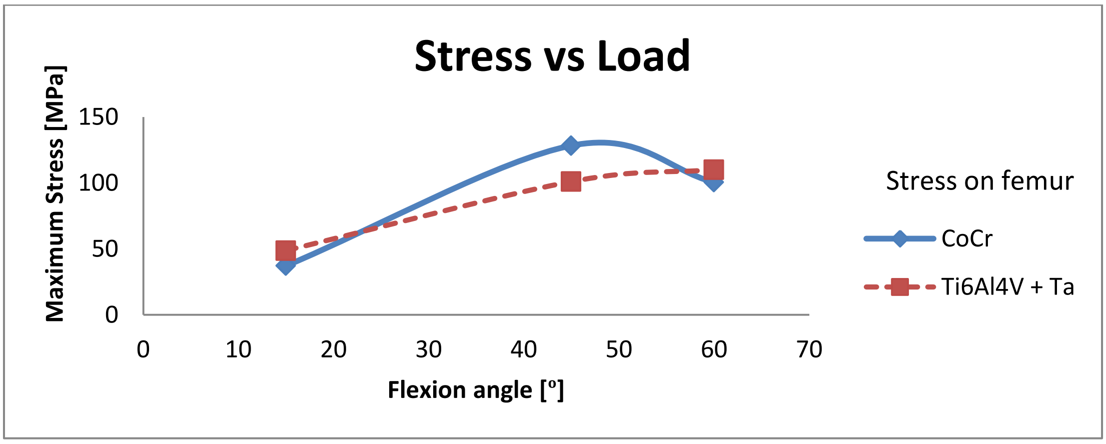

a) Cocr and Ti6Al4V+Ta

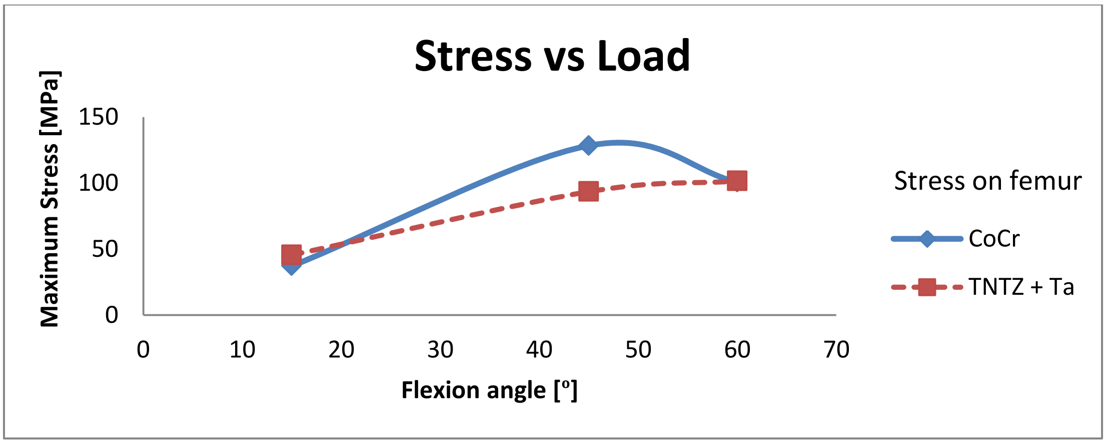

b) Cocr and Ti6Al4V+Ta

Figure 6.2: Comparison of contact stresses on Femoral component

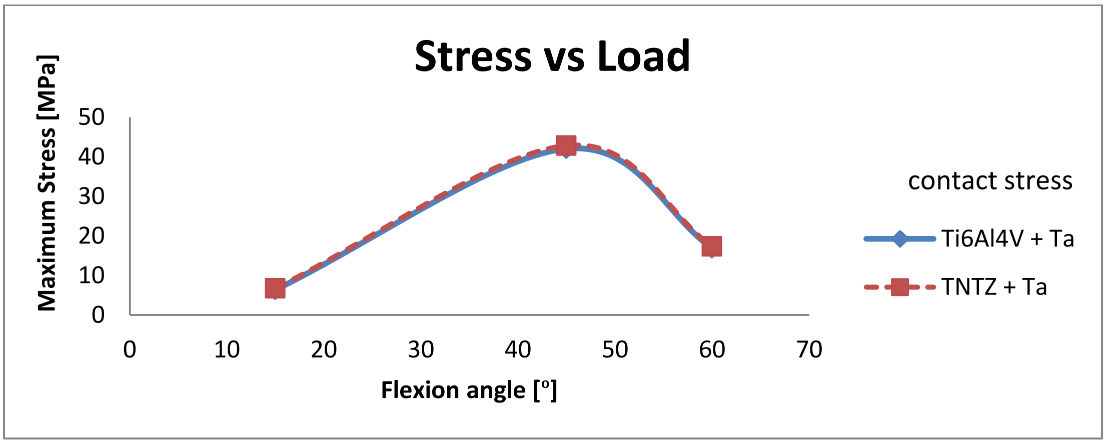

Figure 6.3: Comparison of contact stresses for Case 1 and Case 2

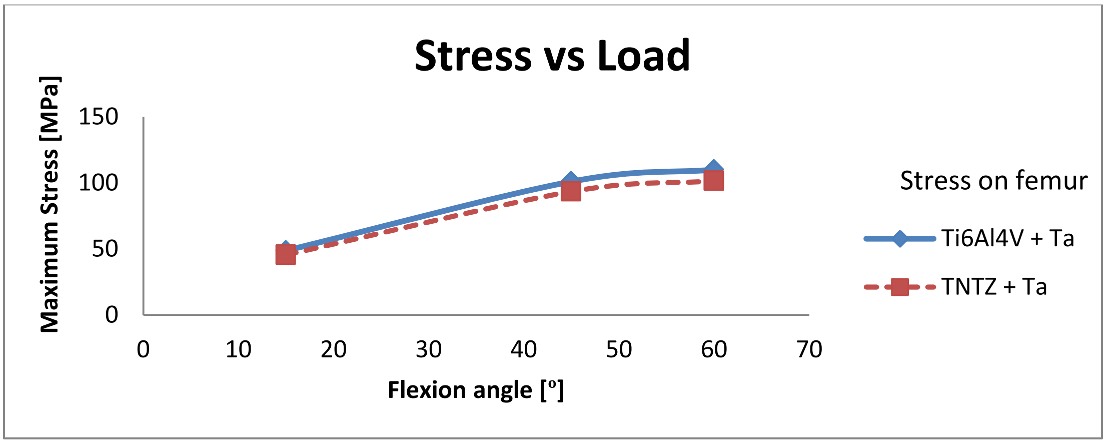

Figure 6.4: Comparison of stresses on Femoral component for Case 1 and Case 2

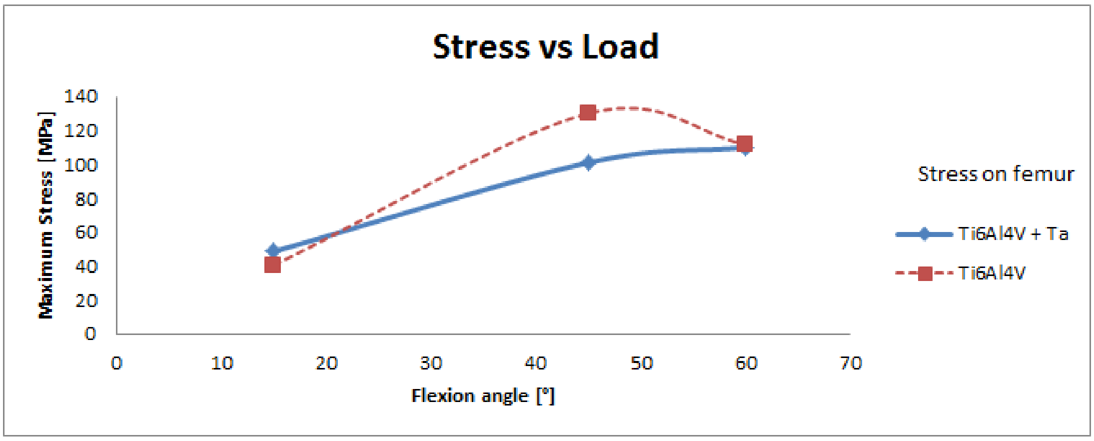

Figure 6.5: Comparison of stresses on Femoral component for New improved implant (Ti6Al4V + Ta) and Solid implant (Ti6Al4V)

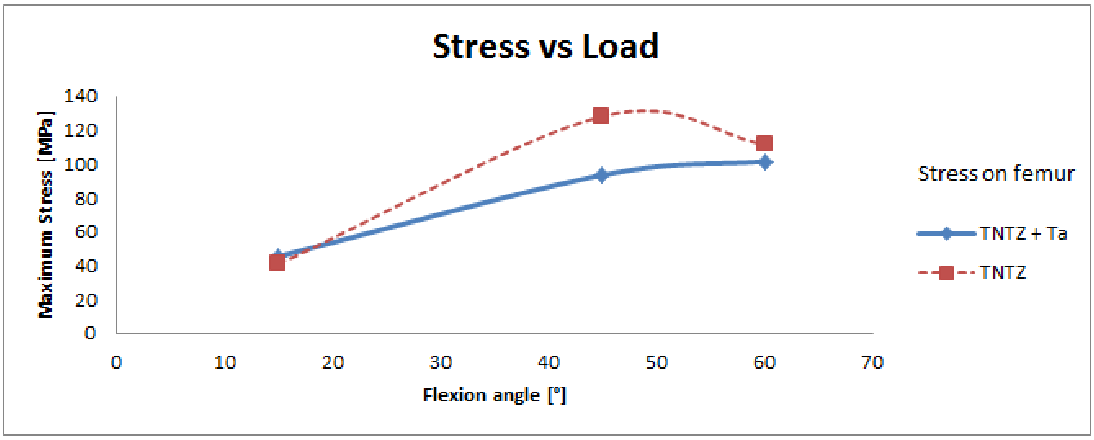

Figure 6.6: Comparison of stresses on Femoral component for New improved implant (TNTZ + Ta) and Solid implant (TNTZ)

The contact stresses on PE insert and the stresses on Femoral component are shown in the Figure 6.7 to Figure 6.10 at various flexion angles and at different loadings.

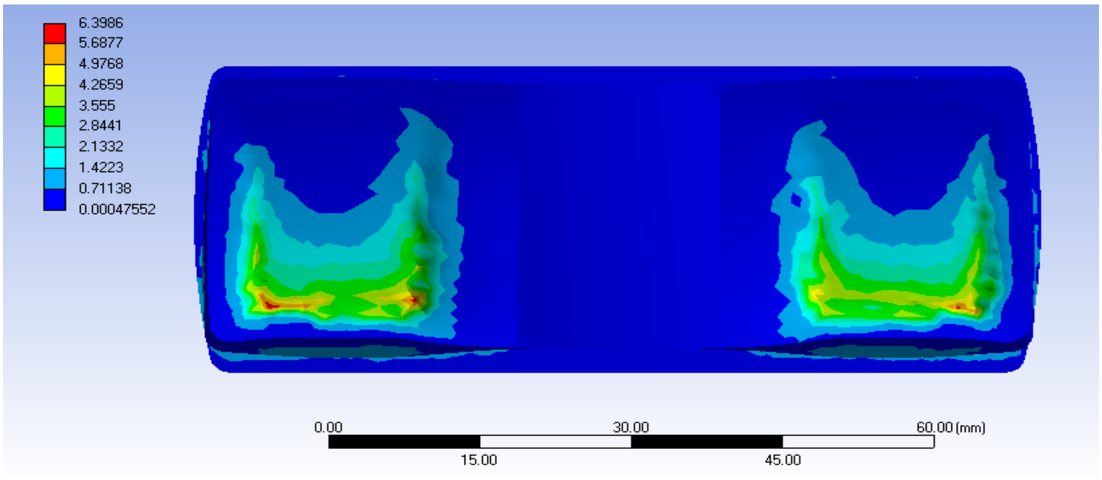

a) 15^{0} Flexion angle

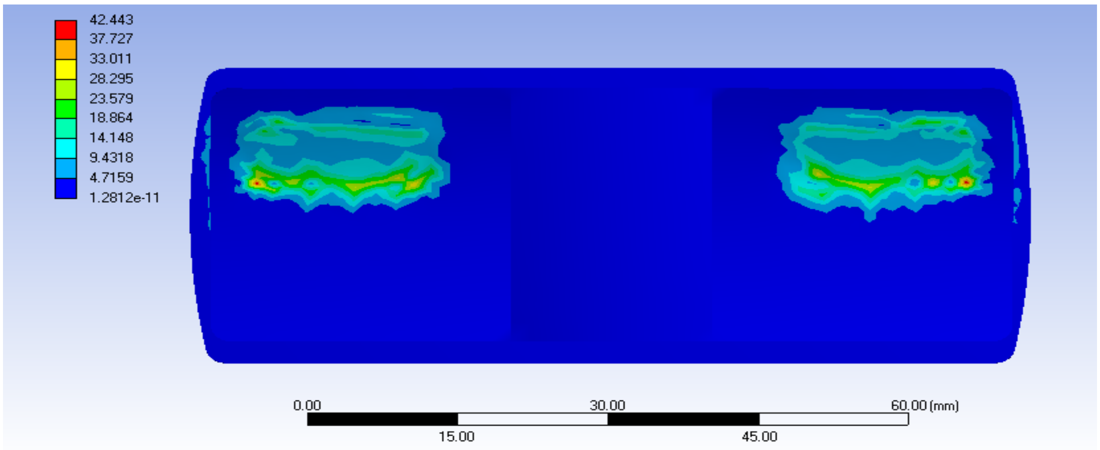

b) 45^{0} Flexion angle

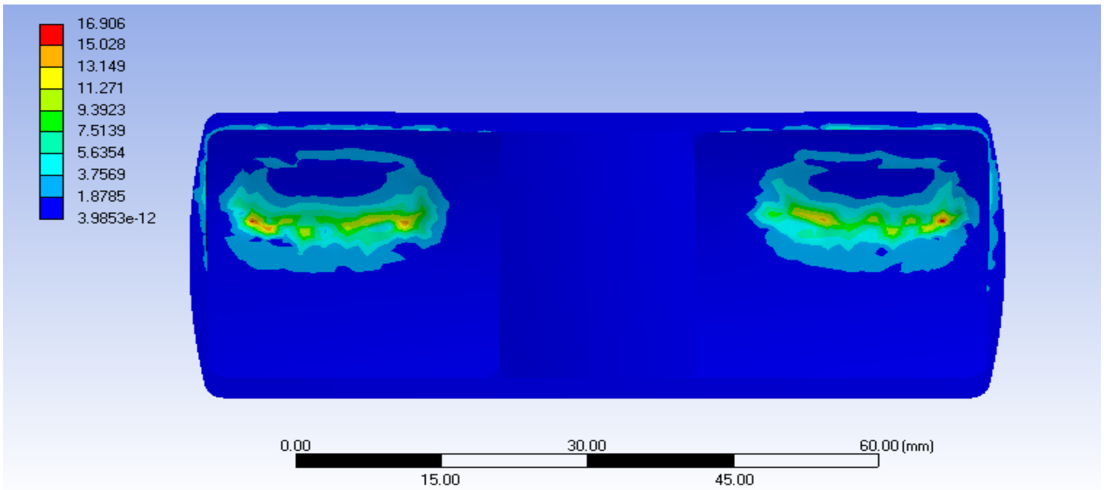

c) 60^{0} Flexion angle

Figure 6.7: Contact stresses on the PE Insert for Case 1.

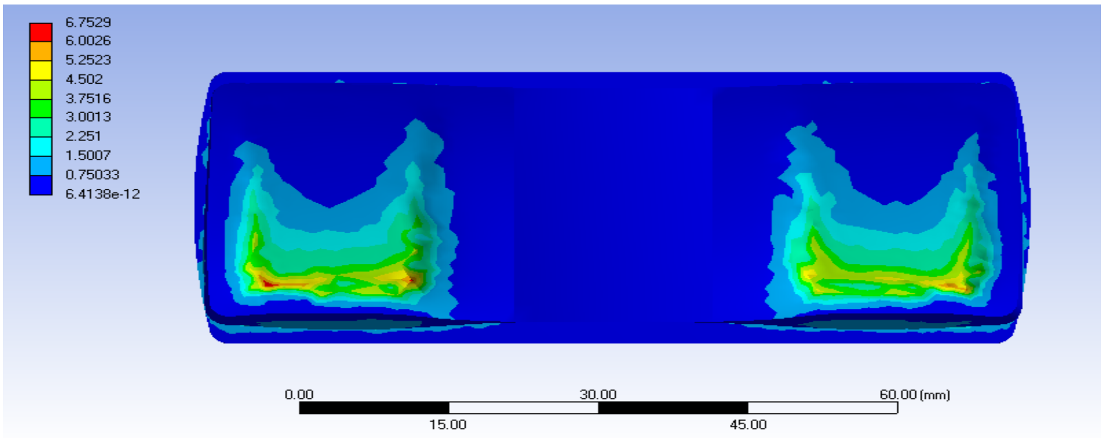

a) 15^0 Flexion angle

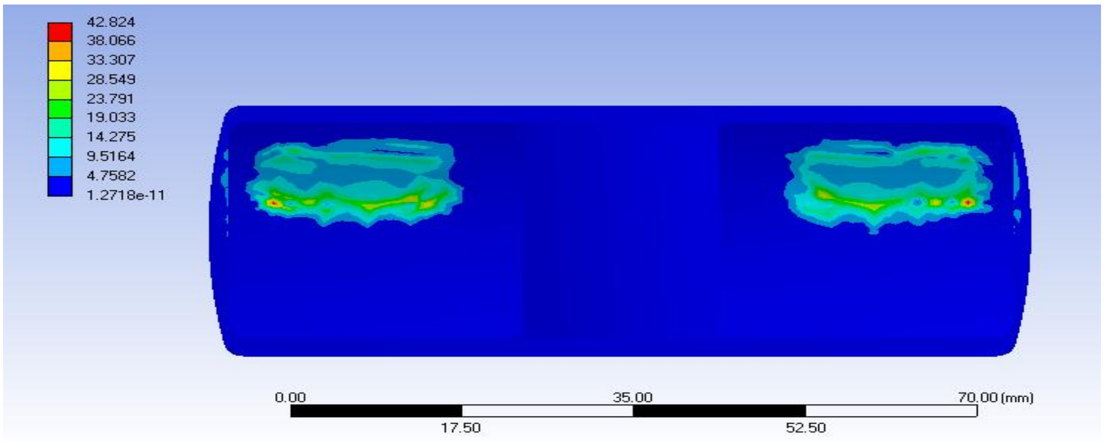

b) 45^0 Flexion angle

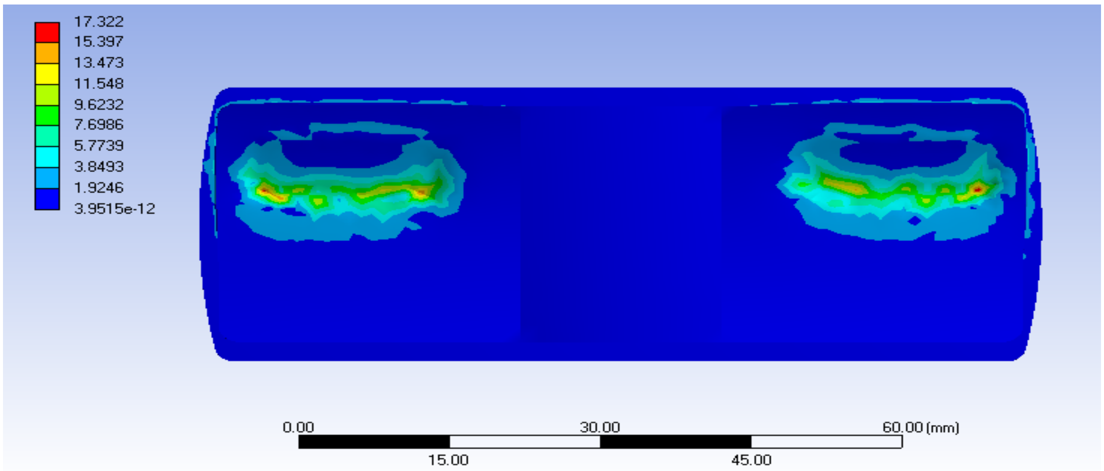

c) 60^0 Flexion angle

Figure 6.8: Contact stresses on the PE Insert for Case 2.

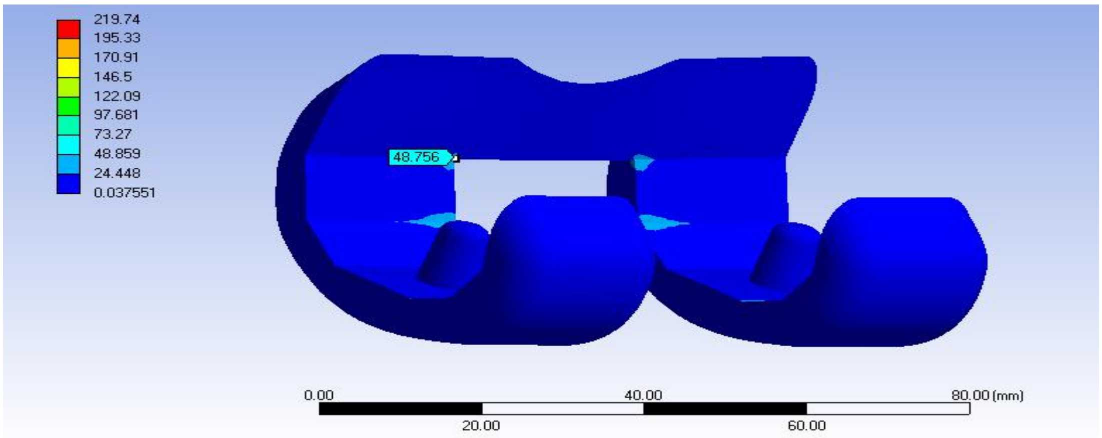

a) 15^0 Flexion angle

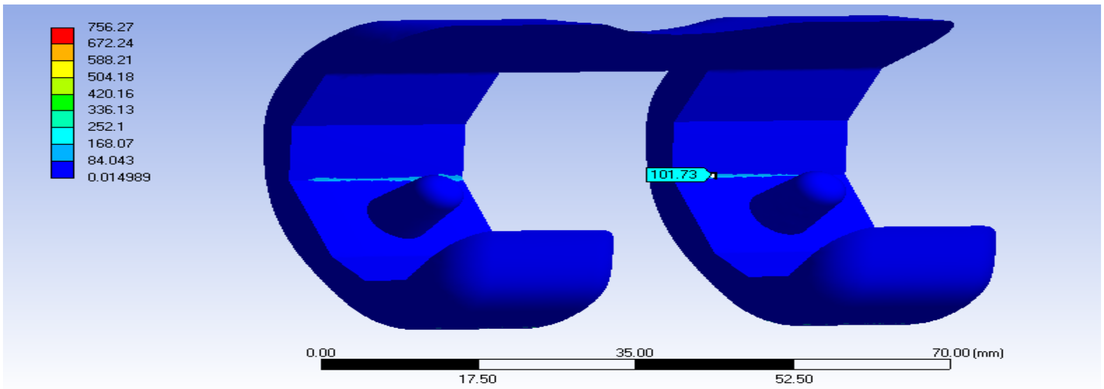

b) 45^0 Flexion angle

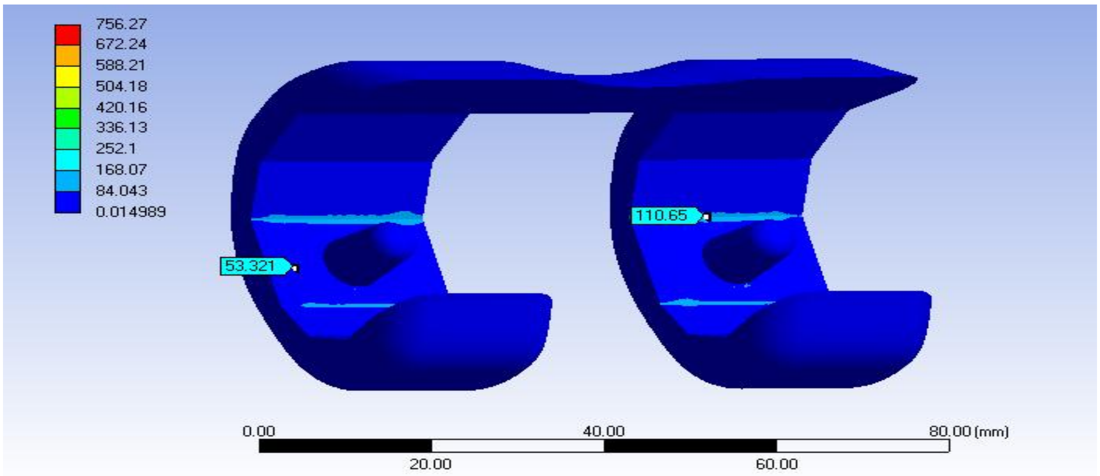

c) 60^0 Flexion angle

Figure 6.9: Stresses on the Femoral component for Case 1.

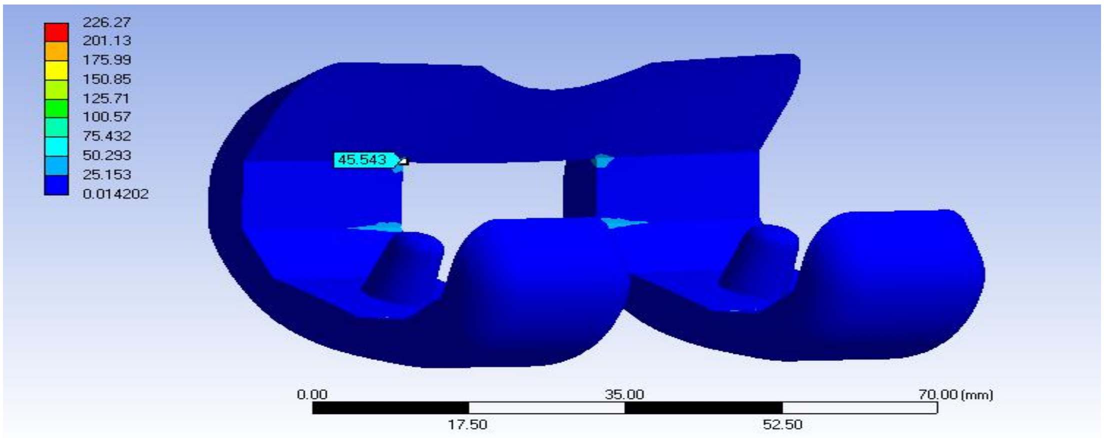

a) 15^0 Flexion angle

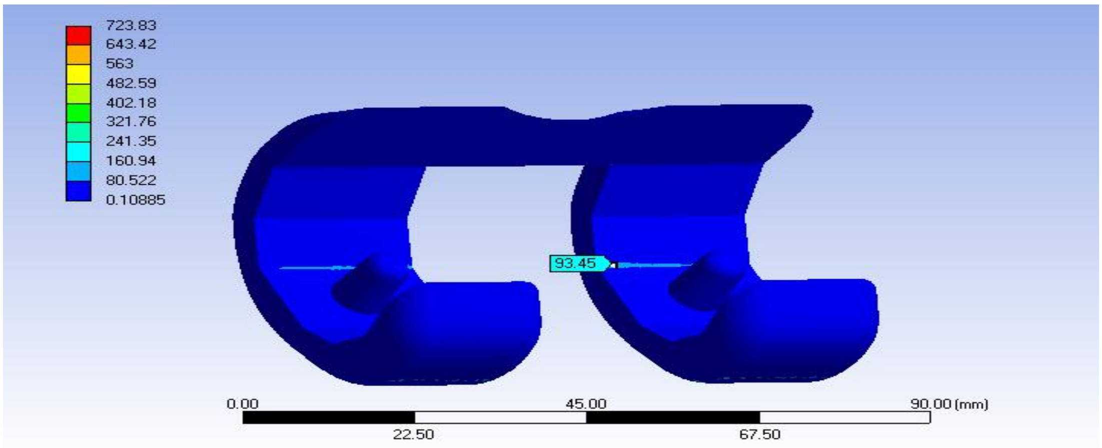

b) 45^0 Flexion angle

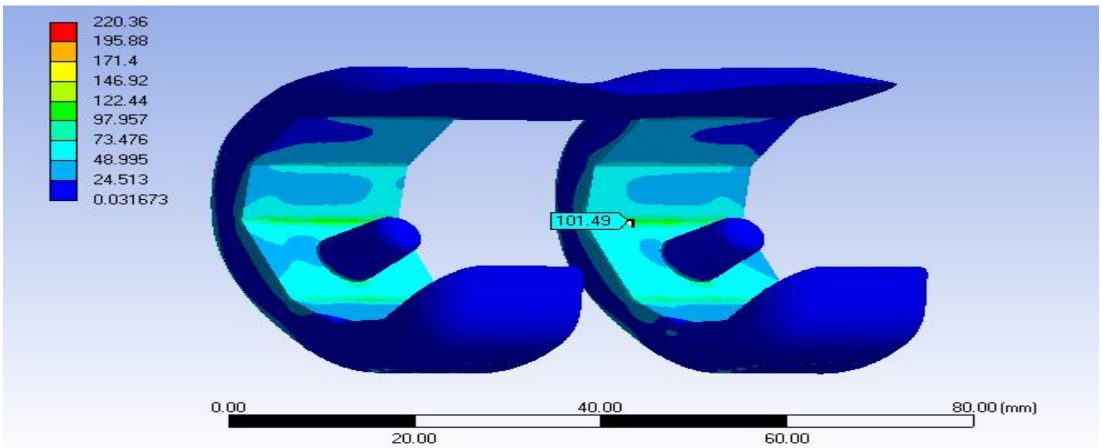

c) 60^0 Flexion angle

Figure 6.10: Stresses on the Femoral component for Case 2.

Chapter 7
Conclusions

The following observations have been made while performing finite element analysis:

1. From the comparison of FEA results with experimental results Figure 6.1, it was observed that the contact stresses are less in the new improved knee joint implant compared to the complete dense implant. This reduction in the contact stresses proves reduction in wear between the Femoral component and PE insert and increases the life of the knee joint implant.

2. It was observed from the Figure 6.2, that the stresses on the Femoral component is reduced compared to the validation results. This indicates the reduction in stress shielding effect and bone resorption between the bone and the Femoral component.

3. By the Improved knee joint implant, the overall weight of the knee joint implant is reduced by 45.87% compared to the implant used by Tomaso et al [18].

7.1 Future Scope

The model which is used in the present thesis is further improved as follows:

1. High stresses are seen in the Femoral component at the edges on the faces, this can be reduced by making the edges curved.

2. In the present research, Titanium and its alloys, Tantalum materials are used for numerical analysis. Further, new materials can be used which reduces the stress shielding effect.

References

[1] Milan H, Ondrej C, Tomas P, Josef S, Martin M, Jindrich N, and J Dvoracek. Medical implants by using RP and investment casting technologies. 1672-6421, (2011) pages 107-111

[2] McKeever DC. Tibial plateau prosthesis. Clin Orthop Rel Res. 192 (1985) pages 3–12.

[3] Utah Hip and Knee Center. http://www.utahhipandknee.com/history.htm.

[4] Robinson RP. The early innovator of today's resurfacing condylar knees. J Arthrop 20 (Suppl. 1), (2005) pages 2–26.

[5] Chu T. An investigation on contact stresses of New Jersey Low Contact Stress (NJLCS) knee using finite element method. J Sys Integr 9 (1999) pages 187–99.

[6] American Academy of Orthopaedic Surgeons. http://www.aaos.org

[7] Brandi C. Carr, Tarun Goswami. Knee Implants- Review of models and biomechanics. Elsevier: Materials and Design 30 (2009) pages 398-413

[8] V.K Balla, P.D DeVasConCellos, W.Xue, Susmita Bose, Amit Bandyopadhyay. Fabrication of compositionally and Structurally graded Ti-TiO_2 structures using Laser Engineered Net Shaping (LENS). Acta Biomaterialia 5 (2009) pages 1831-1837

[9] S.Surya Kumar, K.P Karunakaran, Alain Bernard, U.Chandrasekhar, N.Raghavender. Weld bead modeling and process optimization in Hybrid Layered Manufactruing. Elsevier computer-Aided Design 43 (2011) pages 331-344.

[10] Nagarjan T, Shivalinge Gowda KP, Syed Mansoor Ahmed and S Badami. Rapid Prototyping technique in medical field. J.Pharm. and Tech. 1(4), (2008) pages 341-344.

[11] Gibson, L.K. Cheung, S.P. Chow, W.L Cheung, S.L. Beh, M.Savalani, S.H. Lee. The use of rapid prototyping technology to assist medical applications. AFPR, (2004) pages 1-8.

[12] Di Wu, Qingxi Hu, Gaochun Xu. Study on the application of rapid prototyping in assistant surgical planning. IFMBE proceedings 19 (2008) pages 729-732.

[13] Jelina Milovanovic, Miroslav Trajanovic. Medical applications of rapid prototyping Facta Universitatis 5(1) (2007) pages 79-85.

[14] Sekou Singare, Yaxiong Liu, Dichen Li, Bengheng Lu, Jue Wang, Sanhu He. Individually prefabricated prosthesis for maxilla reconstruction. J. Prosthodontics 1532-849, (2007) pages 1-6.

[15] Jeng-Nan Lee, Hung-Shyong Chen, Chih-Wen Luo and Kuan-Yu Chang. Rapid prototyping and Multi-axis NC machining for the femoral component of knee prosthesis. J. Life Science, 6(3), (2009) pages 73-77.

[16] J.F.I. Saldarriaga, S.C.Velez, and I.E.B.B Henao. Design and manufacturing of a custom skull implant. American J. of Engineering and Applied Sciences 4(1), (2011) pages 169-174.

[17] J. P. Kruth, B. Vandenbroucke, J. Van Varenberg and I. Naert. Rapid manufacturing of dental prosthesis by means of selective laser sintering/melting. Journal of Dental Technology 2007 pages 25-31.

[18] Amit Bandyopadhyay, B.V Krishna, Weichang Xue, Susmita Bose. Application of Laser Engineered Net Shaping (LENS) to manufacture porous and functionally graded structures for load bearing implants. J. Mater Sci: Mater Med (2009) S29 – S34.

[19] Tomaso Villa, Francesco Migliavacca, Dario Gastaldi, Maurizio Clombo and Riccardo Pietrabissa. Conntact stresses and fatigue life in a knee prosthesis: comparision between in vitro measurements and computational simulations. J. of Biomechanics 37 (2004) pages 45-53.

[20] E. Pena, B. Calvo, M.A. Martinez, D. Palanca, M.Doblare. Finite element analysis of the effect of meniccal tears and meniscectomies on human knee biomechanics. Clinical Biomechanics 20(2005) pages 498-507.

[21] Habiba Bouhherara, Ziauddin Mahboob, Milan Miric, Md. Youssef. Finite element investigation of hybried and conventional knee implants. International J. of Engineering 3 (2009) pages 257-264.

[22] M. Sivasankar, V. Mugendiran, S. Venkatesan, A .Velu. Failure analysis of knee prosthesis. Recent Research in Science and Technology 2(6), (2010) pages 100-106.

[23] Bernardo Innocenti, Hans-Peter W. van Jonbergen, Luc Labey and Nico Verdonschot. Periprosthetic stress shielding in patella-femoral arthroplasty: a numerical analysis. SIMULIA Customer Conference, (2011) pages 1-12.

[24] Y.Kalyana Cahkravarthy, D. Suneel and D. Lingaraju. Alternate materials for modeling and analysis of prosthetic knee joint. International J. of Science and Advanced Technology 1(5) (2011) pages 262-266.

[25] M. Niinomi and M. Nakai. Titanium-based biomaterials for preventing stress shielding between implant devices and bone. International J. of Biomaterials, 10.1155, (2011) pages 1-10.

[26] B.R. Levine, Scott Sporer, R.A Poggie, C.J Della Valle, J.J Jacobs. Experimental and clinical performance of porous tantalum in orthopedic surgery. Biomaterials 27 (2006) pages 4671-4681.

[27] Lucy A. Knight, Saikat Pal, John C. Coleman, Fred Bronson, Hani Haider, Danny L. Levine, Mark Taylor, and Paul J. Rullkoetter. Comparison of long-term numerical and experimental total knee replacement wear during simulated gait loading. J. of Biomechanics 40, (200) pages 1550-1558.

[28] C. Shashishekar and C.S. Ramesh. Finite element analysis of prosthetic knee joint using ansys. WIT press 12, (2007) pages 1-8.

[29] Louis E. DeFrate, Hao Sun, Thomas J Gill, Harry E. Rubash, Guoan Li. In Vivo tibiofemoral contact analysis using 3D MRI- based knee models. J. of Biomechanics 37 (2004) pages 1499-1504.

[30] Reilly, D.T. and Burstein, A. H., The elastic and ultimate properties of compact bone tissue, J. Biomechanics , 8 (1975) pages 393-405.

[31] John T S, et. Knee Joint Anatomy. 2011.

[32] Knee replacement: http://bonesmart.org/joint-replacement-surgery/knee.